VOLUME 117, NUMBER 25
JUNE 28, 1995

JOURNAL OF THE AMERICAN CHEMICAL SOCIETY

The Energetics of Helix Formation by Short Templated Peptides in Aqueous Solution. 1. Characterization of the Reporting Helical Template Ac-Hel$_1$

D. S. Kemp,* Thomas J. Allen, and Sherri L. Oslick

Contribution from the Department of Chemistry, Room 18-582, Massachusetts Institute of Technology, Cambridge, Massachusetts 02139

Received September 7, 1994[⊗]

Abstract: Conformational properties obtained from ^{1}H NMR, CD, and molecular mechanics analysis are reported for Ac-Hel$_1$, an N-terminal helix-inducing template for polypeptides. The conformational state ratio [ts]/[cs] of Ac-Hel$_1$ is shown to be 0.79 ± 0.14 in water and in trifluoroethanol−water mixtures. The rate of (t)−(c) state equilibration and the sensitivities of the ([ts] + [te])/[cs] state ratio to salt, temperature, and TFE concentration are reported. The [t]/[c] state ratio is shown to be a reliable monitor of stability of peptide structure induced by Ac-Hel$_1$.

Ac-Hel$_1$ (Figure 1) is the first example of a reporting conformational template, a novel and potentially incisive tool for defining the energetics of short peptide helices in solution.[1,2] In this paper we provide evidence that validates the analytical use of Ac-Hel$_1$.

The reporting features of Ac-Hel$_1$ arise because the conformational changes induced by Ac-Hel$_1$ in a linked peptide are mirrored by complementary and easily measurable changes in the template. In this first of a three-part series we present detailed ^{1}H NMR and molecular mechanics analyses that focus solely on these changes in Ac-Hel$_1$. Here the peptide portion of the conjugate is viewed merely as an agent that induces changes in the relative energetics of the template conformational states. The second paper of this series will examine the peptide and address the complementary structural changes that occur in it when conjugated to Ac-Hel$_1$. A final paper will define and explore the relationship between measurable template properties and the helical stability of the peptide. In subsequent reports we will address the structural and energetic properties of helical alanine-lysine conjugates, the assignment of amino acid *s* values from properties of host−guest alanine-lysine-derived peptides, and the effects of trifluoroethanol−water mixtures on peptide helicity.

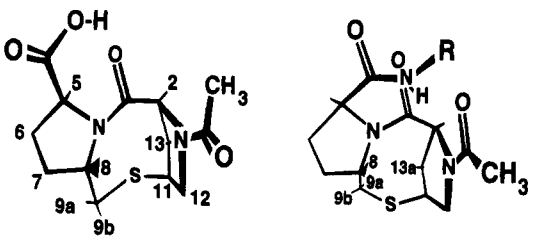

Figure 1. Structure and site numbering of the helical template Ac-Hel$_1$. Left: X-ray crystal structure of Ac-Hel$_1$-OH, (cs) conformation. Right: MM structure of Ac-Hel$_1$-NHR, (te) conformation.

For a simple polypeptide in aqueous solution the spontaneous initiation of local helical structure is highly improbable,[3] with the consequence that most short peptides lack detectable helical

⊗ Abstract published in *Advance ACS Abstracts*, May 15, 1995.

(1) Kemp, D. S.; Curran, T. P.; Davis, W. M.; Boyd, J. G.; Muendel, C. C. *J. Org. Chem.* **1991**, *56*, 6672−6682. Kemp, D. S.; Curran, T. P.; Boyd, J. G.; Allen, T. *J. Org. Chem.* **1991**, *56*, 6683−6694. Kemp, D. S.; Curran, T. P. *Tetrahedron Lett.* **1988**, *29*, 4935.

(2) Kemp, D. S.; Boyd, J. G.; Muendel, C. C. *Nature* **1991**, *352*, 451−454. Kemp, D. S.; Allen, T.; Oslick, S. *Peptides, Chemistry, Structure, Biology*; Smith, J., Rivier, J., Eds.; ESCOM: Leiden, 1992; pp 353−355.

(3) Poland, D.; Scheraga, H. S. *Theory of the Helix−Coil Transitions in Biopolymers*; Academic Press: New York, 1970.

0002-7863/95/1517-6641$09.00/0

structure. Efficient initiation of helices can be achieved by addition of helix-enforcing local constraints in the form of covalent bonds between peptide side chain functions[4] or by linkages to terminal capping functions that present hydrogen bonding sites in a helical array.[5] Work in a number of laboratories has shown that these templating principles permit induction of helicity in peptides that would otherwise be randomly structured.[1,4,5] Studies of templated helices have significant biological relevance since low molecular weight peptides that assume helical conformations find application in the design of versatile bioorganic frameworks and in drug design.[4]

We have coined the term "reporting conformational template" (RCT), to describe an agent that when linked to an otherwise unstructured polymer both initiates structure and signals its own act of initiation.[1] Because an RCT reports a local conformational property, it is likely to provide structural and energetic insights that are complementary to those from more conventional global characterization techniques such as denaturation, melting behavior, or circular dichroism spectroscopy (CD). Full energetic characterization of peptide helices in solution has high priority for the protein folding problem, since helices are often formed early in the folding of the primary amino acid sequence of globular proteins.[6] Moreover, given doubts that have recently been expressed concerning the generality of conclusions deduced from existing helical models,[7,8] new tools for energetic characterization of isolated helices in solution are opportune.

Conformational Properties of Derivatives of the RCT Ac-Hel$_1$

We have previously reported convergent syntheses[1,9] of the RCT Ac-Hel$_1$-OH and using ^{1}H NMR spectroscopy have characterized its N-templated polyalanine conjugates as helical in nonaqueous media.[1] We have also briefly described their aqueous behavior.[2] The acid Ac-Hel$_1$-OH and its ester have been shown to exist in a variety of organic solvents as an equilibrated mixture of two conformational states resulting from 180° rotation at the acetyl amide bond. These cs and ts states are shown in Figure 2 (the c and t identifies refer to the *s-cis*- and *s-trans*-amide conformations, respectively).[10] For one

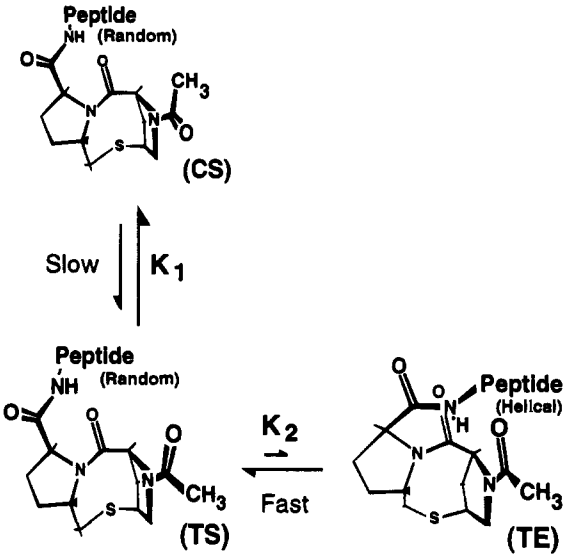

Figure 2. Dynamic equilibrium in solution of Ac-Hel$_1$-peptide conjugates as established by ^{1}H NMR spectroscopy. Illustrated structures correspond to MM energy minima.

crystalline form of Ac-Hel$_1$-OH the cs state has been characterized by X-ray diffraction; (cs) is also the single state observed by ^{1}H NMR for Ac-Hel$_1$-OMe in $CDCl_3$ solution.[1] Owing to slow rotation about the amide bond, the (c) and (t) states generate separately detectable NMR resonances, which have been assigned unambiguously by COSY and NOE analyses.

The presence of a third conformational state (te) is revealed through study in solution of Ac-Hel$_1$-peptide conjugates. This state corresponds to a reorientation of the thioether bridge for the t state amide conformer (the s and e identifiers refer to the staggered or partially eclipsed orientation at the C-8−C-9 C−C bond). Since derivatives of Ac-Hel$_1$ that lack the capacity to form intramolecular hydrogen bonds show only the s state NMR signature, the lactam thioether e state must be the less stable of the two and must be selectively stabilized to become detectable. Studies of Ac-Hel$_1$-peptide conjugates in organic solvents imply that the te state is unique in initiating helices efficiently. Since the (s) and (e) states are in rapid equilibrium on the NMR time scale, (t) state resonances must correspond to a (ts)−(te) state average, and (t) state chemical shifts and coupling constants are abundance-weighted averages of limiting (ts) and (te) values. A selective increase in the stability of a template-nucleated peptide helix thus results in two changes in the template resonances: (1) an increase in the ratio of integrated intensities of the separate resonances attributable to (t) versus (c) states, and (2) an increase in te character of the (ts)−(te) state average.

Scope of This Report

For aqueous solutions the fractional helicity of helical peptides and proteins has been shown to be significantly influenced by changes in temperature and in the concentration of salt and additives such as alcohols.[11,12] Determination of the sensitivity of the template [t]/[c] ratio to these changes is therefore an essential part of the characterization of this functionality as an RCT. These measurements are reported herein for simple Ac-

(4) Felix, A. M.; Heimer, E. P.; Wang, C.-T.; Lambros, T. J.; Fournier, A.; Mowles, T. F.; Maines, S.; Campbell, R. M.; Wegrzynski, B. B.; Toome, V.; Fry, D.; Madison, V. S. *Int. J. Peptide Protein Res.* **1988**, *32*, 441−454. Osapay, G.; Taylor, J. W. *J. Am. Chem. Soc.* **1992**, *114*, 6966−6973. Ruan, F.; Chen, Y.; Hopkins, P. B. *J. Am. Chem. Soc.* **1990**, *112*, 9403−9404. Ghadiri, M. R.; Choi, C. *J. Am. Chem. Soc.* **1990**, *112*, 1630−1632. Ghadiri, M. R.; Soares, C.; Choi, C. *J. Am. Chem. Soc.* **1992**, *114*, 4000−4002. Jackson, D. Y.; King, D. S.; Chmielewski, J.; Singh, S.; Schultz, P. G. *J. Am. Chem. Soc.* **1991**, *113*, 9391−9392.

(5) Arrhenius, T.; Lerner, R. A.; Satterthwait, A. C. *UCLA Symp. Mol. Cell Biol. New Ser.* **1987**, *69*, 453−457. Mueller, K.; Obrecht, D.; Knierzinger, A.; Stankovic, C.; Spiegler, C.; Bannwarth, W.; Trzeciak, A.; Englert, G.; Labhardt, A. M.; Schoenholzer, P. In *Perspectives in Medicinal Chemistry*; Testa, B., Kyburz, E., Fuhrer, W., Giger, R., Eds.; VCH: Weinheim, New York, 1993; Chapter 33, pp 513−531.

(6) Serrano, L.; Neira, J.-L.; Sancho, J.; Fersht, A. R. *Nature* **1992**, *356*, 453−455.

(7) Lesk, A. M. *Nature* **1991**, *352*, 379−380.

(8) Sancho, J.; Neira, J. L.; Fersht, A. R. *J. Mol. Biol.* **1992**, *224*, 749−758. Hughson, F. M.; Barrick, D.; Baldwin, R. L. *Biochemistry* **1991**, *30*, 4113−4118. Eloeve, G. A.; Chaffotte, A. F.; Roder, H.; Goldberg, M. E. *Biochemistry* **1992**, *31*, 6876−6883.

(9) McClure, K.; Renold, P.; Kemp, D. S. *J. Org. Chem.* **1995**, *60*, 454−457.

(10) Glossary of abbreviations and terms: TFE, trifluoroethanol; RCT, reporting conformational template; MM, molecular mechanics modeling; t, the acetamido-s-*trans* conformational state; c, the acetamido-s-*cis* conformational state; s, the conformational state with the C8−C9 bond in a near-staggered orientation; e, the conformational state with the C8−C9 bond in a near-eclipsed orientation; (t) the manifold consisting of all conformations of a molecule that share the t conformational state; (te), the manifold consisting of all conformations of a molecule that share both the t and the e conformational states; [t] the molar concentration of all conformations that share the t conformational state; CC, correlation coefficient. Unless otherwise noted, all structural representations correspond to MM minimized conformations.

(11) von Hippel, P. H.; Wong, K.-Y. *J. Biol. Chem.* **1965**, *246*, 3909−3923. Brown, J. E.; Klee, W. A. *Biochemistry* **1971**, *10*, 470−476.

(12) Klee, W. A. *Biochemistry* **1968**, *7*, 2731−2736. Nelson, J. W.; Kallenbach, N. R. *Proteins* **1986**, *1*, 211−217.

Hel$_1$ derivatives, along with rate measurements that define their kinetic properties.

Before the template [t]/[c] ratio can be used as a reliable measure of peptide helicity in the (te) state, it is necessary to demonstrate that the (cs) state used as an energetic reference does not induce unique length-dependent template-initiated structure in the linked polypeptide. This key issue is explored in the context of the demonstration of a simple empirical relationship between the [t]/[c] state ratio and the fractional s-e character of the (t) state. A combination of empirical results and a complete molecular mechanics characterization of Ac-Hel$_1$ leads to the conclusion that the reporting features of the Ac-Hel$_1$-peptide conjugates are defined by hydrogen bonding interactions between the template acetamido function and the first two N-terminal peptide residues.

Helices that are initiated in polypeptides by linked N- or C-terminal RCTs have special structural and energetic features that must be taken into account when drawing a comparison with helices formed in isolated polypeptides by spontaneous initiation. As a prelude to the subsequent discussions of the papers in this series, these features are discussed in the next section.

Structural and Energetic Characterization of Template-Nucleated Helices—Helical Cooperativity

The helical structure of an Ac-Hel$_1$-peptide conjugate differs from that expected for a simple helical peptide that obeys classical models for helicity.[3] The number of significant helical substates are far fewer, the relationship between their structures is simpler, and the calculation of energetics from [t]/[c] ratio measurements is therefore distinct. The length dependence of helical energetics in turn affects the nature of the cooperativity that can be expected for a templated helix. These issues are fundamental to all applications of helix-inducing RCTs.

Helix−coil interconversions are very rapid, allowing subspecies concentrations to be modeled by mass action relationships.[13] In the absence of very significant local stabilizing factors, the stability of short helices formed from unaggregated simple peptides in water is marginal, and the structure must be viewed as a manifold containing many nearly isoenergetic, rapidly equilibrating conformations. Thermodynamic models for the helix−coil interconversion usually postulate an initiation parameter σ, which reflects the difficulty of enforcing a helical conformation at each of six single bonds of three contiguous peptide residues, and a propagation parameter s, which reflects the tendency of a single amino acid residue linked to a helical region to forgo a random orientation and join the preexisting helix.[14,15] Although σ is assignable experimentally from the melting curves of oligopeptides,[16] for the analysis of helicity of small peptides it is usually assumed to be temperature-independent and to lie in the range of 5×10^{-3} to 10^{-4}, found from oligopeptide studies.[17,18] Under the usual assumption that σ is independent of local amino acid sequence, a consequence of a small σ is that a particular peptide molecule of length n contains only one helical region of variable length, which may appear anywhere within the chain.[3] The resulting state sum is complex, and calculation of fractional helicity for unaggregated helical peptides has usually been carried out with Ising model-derived partition functions of the Zimm−Bragg[14] or Lifson−Roig[15] type. Under the above assumptions, these have been used to fit s values to experimentally observed helicity.[17,19]

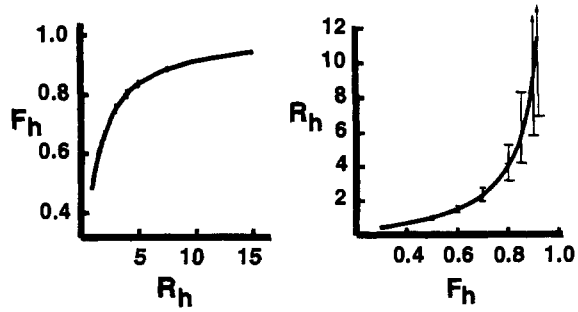

Figure 3. Left: Simulated calculation of fractional helicity F_h from the helical ratio R_h using $F_h = R_h/(1 + R_h)$. Right: Simulated calculation of helical ratio R_h from the fractional helicity F_h using $R_h = F_h/(1 - F_h)$. Error bars in each graph correspond to an assumed ±5% relative error in each abscissa value.

Since an RCT is likely to overwhelm intrinsic initiation propensities, helicity analyses of peptides bearing N- or C-terminal RCTs offer a conceptually and algebraically simpler alternative that carries fewer assumptions. Provided the templated peptide length is less than *ca.* 20 residues and the initiation parameter for the template is 1−2 orders of magnitude greater than the largest peptide-derived σ, the templated helical peptide must be a manifold of helical conformations of varying length, all of which propagate outward from the template−peptide junction. If structure is defined as fractional helicity at a given amino acid site, a templated helical peptide must show maximum structure proximal to the template and minimum structure distal to the template. For homopeptides the mass action expression describing the overall fractional helical character then approximates a linear function of a simple geometric series in the propagation factor s.[1]

A pivotal issue in quantitating helicity is the nature of the reporting measurement. Most physical methods monitor fractional helical character. Unfortunately this is a less incisive property than the ratio of abundances of helical and nonhelical states. A two-state model clarifies this point. If c and h refer respectively to coil (nonhelical) and helical states, fractional helicity F_h and the helical ratio R_h are defined as $F_h = [h]/([h] + [c])$ and $R_h = [h]/[c]$. These ratios are linked by the following simple expressions, $F_h = R_h/(1 + R_h)$ and $R_h = F_h/(1 - F_h)$, and might be expected to be computationally equivalent. However, F_h and R_h are equivalent only in the absence of significant experimental error. As shown by the graph of Figure 3, the calculation of accurate R_h values from F_h values that exceed 0.8 requires unattainably high experimental precision, while the reverse calculation is much less error-prone. Given likely experimental errors, R_h is thus the more valuable parameter. In the third paper of this series it will be shown that for the RCT Ac-Hel$_1$, R_h can be related to the ratios of integrated areas of two sets of NMR resonances corresponding to peptides in helical and nonhelical conformations. Given normal integration errors, this ratio is well defined in the range of 0.1 to 10, and ratios in the range of 0.03 to 0.1 and 10 to 30 can be approximated with some loss of precision.

Cooperativity[20] is often viewed as a key feature of the protein folding process, and the spontaneous formation of helices in

(13) Schwartz, G. *J. Mol. Biol.* **1963**, *15*, 284−297.
(14) Zimm, B. H.; Bragg, J. *J. Chem. Phys.* **1959**, *31*, 526. Zimm, B. H.; Doty, P.; Iso, K. *Proc. Natl. Acad. Sci. U.S.A.* **1956**, *78*, 498.
(15) Lifson, S.; Roig, A. *J. Chem. Phys.* **1961**, *34*, 1963−1974.
(16) Scheraga, H. A. *Pure Appl. Chem.* **1978**, *30*, 315. Wojcik, J.; Altmann, K.-H.; Scheraga, H. A. *Biopolymers* **1990**, *30*, 121−134.
(17) Chakrabartty, A.; Schellman, J. A.; Baldwin, R. L. *Nature* **1991**, *351*, 586−588.
(18) Merutka, G.; Lipton, W.; Shalongo, W.; Park, S.-H.; Stellwagen, E. *Biochemistry* **1990**, *29*, 7511−7515.
(19) Lyu, P. C.; Liff, M. I.; Marky, L. A.; Kallenbach, N. R. *Science* **1990**, *250*, 669−673. Gans, P. J.; Lyu, P. C.; Manning, M. C.; Woody, R. W.; Kallenbach, N. R. *Biopolymers* **1993**, *33*, 1605−1614.
(20) Dill, K. A.; Shortle, D. *Annu. Rev. Biochem.* **1991**, *60*, 795−825. Gill, S. J.; Connelly, P. R.; DiCera, E.; Robert, C. H. *Biophys. Chem.* **1988**, *30*, 133−141.

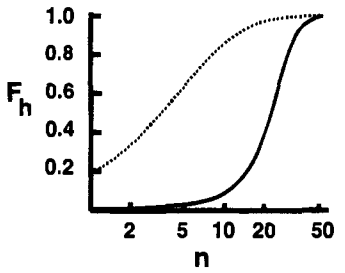

Figure 4. Calculated fractional helicity F_h for a peptide of length n assuming helix initiation solely at the N-terminus and an s value of 1.2. The dotted line corresponds to $\sigma = 0.2$ (efficient initiation). The solid line corresponds to $\sigma = 0.003$ (inefficient nucleation). $F_h = \sigma s(s^n - 1)/s - 1)$.

isolated polypeptides has also been taken to have cooperative character. What is the anticipated effect on helical cooperativity of helix induction by a template? Consider a model in which a homopeptide helix is initiated from one end and propagated with $s = 1.2$, without other stabilizing features. (The inclusion of helices randomly initiated at other sites does not affect this analysis significantly.) Plots of fractional helicity F_h as a function of chain length are shown in Figure 4, both for strong and for very weak N-terminal initiation signals. Experimentally defined cooperative phenomena are often signaled by the abrupt appearance of structure with minimal change in an experimental variable. Taken in this sense the semilogarithmic plot of Figure 4 does indeed give the weak initiation case the appearance of experimental cooperativity. In fact this appearance is largely an artifact of the need to compress the scale of length n, since the additional helical residues that must be added to the chain to change the fractional helicity from barely detectable (0.20) to nearly complete (0.90) are similar in the strong and weak cases ($n = 1$ to 12 for $\sigma = 0.2$, and $n = 15$ to 34 for $\sigma = 0.003$). The large increase in σ has merely shifted the experimentally detectable minimum helical length from medium (15−40 residues) to small (3−15 residues). As expected for an assumed s value only slightly larger than 1, both helices are frayed conformational manifolds and lack the robust structure characteristic of a typical protein in its native state. Neither exhibits the special all-or-nearly-none features of cooperativity that characterize global protein folding.[20]

In the following sense, the high σ case can, however, be viewed as less cooperative. Since σ defines the minimum length n of a peptide for which helicity can be demonstrated, it also defines the minimum number of propagation steps required for detectability helicity. Each such step is characterized by an s that shows a small but defined sensitivity to environmental variables such as temperature and denaturant concentration. The energy of a detectable helix formed with the smaller σ must be a linear function of more s-derived energy terms. Although the effect is not expected to be dramatic, a small σ must thus describe a necessarily longer peptide sequence with a more temperature- or denaturant-sensitive helicity than is seen for a shorter template-nucleated helix, characterized by a substantially larger σ. However, neither model exhibits cooperativity that owes its origin to a tightly articulated set of mutually stabilizing interactions of the type found in native proteins; such cooperativity can only be found in a helix that is stabilized by medium- or long-range inter- or intrahelical interactions.

Background and Molecular Mechanics Analysis

On the NMR time scale the (c) and (t) states each correspond to a manifold of rapidly equilibrating conformational substates. As a first step toward structural understanding of template function, they have been subjected to molecular mechanics analysis. Inspection of simple space-filling models reveals that the rigidity of the molecular framework of Ac-Hel$_1$ restricts conformational states to a pair of alternative choices for each of four variables. In addition to the c/t and s/e state choices, the C6 methylene can assume "in" and "out" puckered orientations, and at the C5−CO single bond the ψ torsional angle can assume helical or extended orientations, as predicted from a Ramachandran diagram. Calculated energies for the significant conformational substates of the amide Ac-Hel$_1$-NHMe and the ester Ac-Hel$_1$-OMe are shown in Table 1.

Table 1. MM-Calculated Properties of Conformational Substates of Ac-Hel$_1$-NHMe and Ac-Hel$_1$-OMe

c/t	s/e	C6 CH_2	C5 ψ angle, deg	calculated E, kcal/mol	NH- - -O distance, Å
			1.Ac-Hel$_1$-NHMe Substates		
t	s	out	−4.9	+3.6	2.22
t	s	out	+108	+3.7	
t	s	in		+7.8	
c	s	out	−0.5	+7.6	
c	s	out	+122	+1.6	
c	s	in	+122	+4.1	
t	e	out	+0.6	−3.2	1.99
t	e	out	+104	−2.3	
t	e	in	+104	−0.7	
			2.Ac-Hel$_1$-OMe Substates		
t	s	out	−30.5	−0.6	
t	s	out	+150	+2.5	
c	s	out	−30	−0.7	
c	s	out	+166	+1.4	
t	e	out	−30	−6.1	

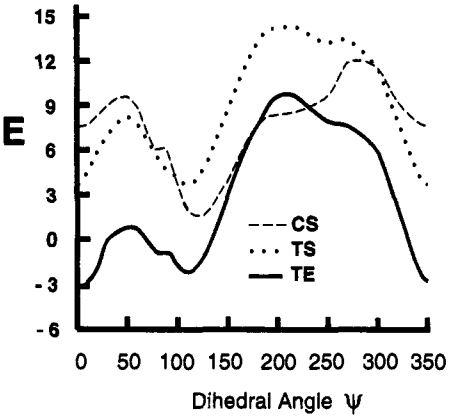

Figure 5. Molecular mechanics calculated torsional energies for rotation about the C5−CO ψ bond for the (cs), (ts), and (te) states of Ac-Hel$_1$-NHMe.

The CH_2 "out" states at C6 are calculated to be 2.5−4 kcal/mol more stable than the "in" states, and we neglect these as pertinent conformers. For the two C5 ψ torsional states of Ac-Hel$_1$-OMe, the extended conformation which directs the peptide chain away from the core of the template (ψ +95 to +70°) is less stable by 2.5−3 kcal/mol than the compact conformation which is potentially helical (ψ 0 to −30°). As seen in Figure 5, for the Ac-Hel$_1$-NHMe ψ conformers, this stability order holds only for the te state. For the cs state the extended conformation is the more stable, while for the ts state the two are calculated to be nearly isoenergetic.

Are s and e unique descriptors of the S−CH_2 conformations? By MM, the internal amide and two pyrrolidine linkages constrain the lactam ring to two well-defined energy minima that are separated by a low-energy maximum (respective torsional angles (4 8, 9 10) and (9 10, 11 13): −87° and +61°; E_{min} = +4.6 kcal/mol). The s and e states must be complete descriptors of Ac-Hel$_1$ conformational space.

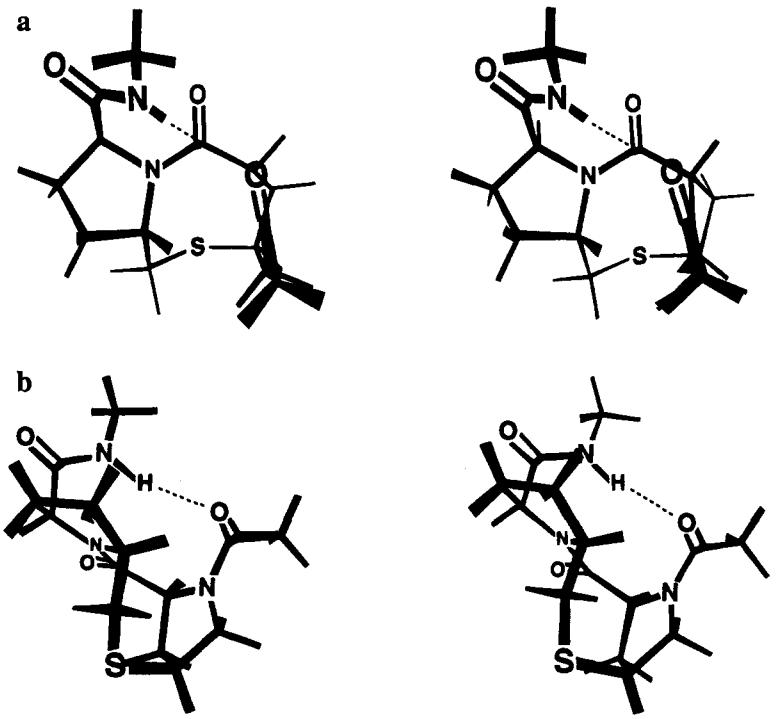

Figure 6. Stereodiagrams of the hydrogen bond of Ac-Hel$_1$-NHMe (MM minimized): (a) sight down the Ac—N amide bond showing the out-of-plane NC,OH dihedral angle; (b) view of the NHO and HOC angles of the hydrogen bond.

How reliable are the energetic estimates of Table 1? Contrary to experiment, an e state is calculated to be more stable than an s, but this comparison is probably the most stringent that can be applied among conformations of Ac-Hel$_1$, whose thialactam ring shows substantial distortions from normal bond angles.[1] Accordingly, angular and torsional strain energies for this region are unlikely to be modeled accurately by the simple angular or torsional potential functions found in most MM software. As a result, calculations of the energy of an Ac-Hel$_1$ conformer, relative to an unstrained reference molecule, will almost certainly contain substantial error, as will comparisons between conformations that dramatically alter core geometry. By contrast, comparisons between conformers with nearly identical core geometries are expected to be much more reliable, particularly since Ac-Hel$_1$ derivatives are exceptionally compact, with low surface-to-volume ratios that should minimize solvation effects.

Of the four state choices, only the s/e dramatically alters the atom positions of the molecular core. The point can be verified by optimally superimposing pairs of structures and calculating a root-mean-square (rms) distance for the resulting 13 pairs of framework atoms. For the cs and ts states of Figure 2, the rms framework deviation is only 0.05 Å, implying that reorientation at the acetamide N—CO bond has negligible structural consequences in the rest of the molecule. For the pairs of C5 ψ torsional orientations corresponding to energy minima (Table 1) the following rms framework deviations are noted: cs, 0.09 Å; ts, 0.08 Å; te, 0.10 Å. By contrast, the ts and te states of Ac-Hel$_1$-NHMe in which the C5 pyrrolidine atoms are optimally paired show an rms deviation of 0.51 Å. Here the local rms deviation for the five C5 pyrrolidine atoms is only 0.08 Å, while for the five C2 pyrrolidine atoms it is 0.63 Å. It is therefore not surprising that the MM-calculated order of energies for the ts and te states is the reverse of experiment. Comparisons within either the s or the e regimes should lack these errors. In studies with close structural analogs of Ac-Hel$_1$-, we have found that if core geometry is preserved, energetic comparisons of conformers show excellent agreement between calculation and experiment.[21]

For compact molecules like Ac-Hel$_1$-, the most reliable prediction of a MM calculation is the molecular structure. A structure is defined by bond distances which change little with minimization and by qualitative trade-offs between the other energetic factors, rather than by their precise magnitudes. We have used different MM protocols and observed essentially invariant geometries for the Ac-Hel$_1$ conformers, despite significant variations in relative and absolute MM-calculated energies. In this analysis, we place primary weight on structural evidence. Comparison of the MM-calculated structure for the cs state of Ac-Hel$_1$- with that obtained from X-ray diffraction analysis of the crystal shows an rms deviation of positions of framework atoms of only 0.07 Å; strikingly, nearly precise superimposition of corresponding atoms was seen for the pendant substitutents at C-1 and C-5 as well as for the molecular core.[1] This result validates our use of MM-derived structural evidence.

The relative strengths of intramolecular amide—amide hydrogen bonds are likely to mediate the s → e state change, and the structural parameters of these bonds are central to an analysis of Ac-Hel$_1$. Literature data correlate the features of commonly encountered amide—amide hydrogen bonds of helices in proteins.[22] The mean values of these, with standard deviations, are the following: O···H bond length, 2.05(0.15) Å; NH—O bond angle, 157(9)°; and H—O=C bond angle, 147(7)°. Although the hydrogen bonds calculated for Ac-Hel$_1$-NHMe are neither colinear nor formed between coplanar amide residues, the NH—O angles calculated for ts and te are respectively 155° and 153°, close to the average of 157° found for helices in proteins, and the H—O=C angles are 118° and 125°, close to

(21) Kemp, D. S.; Rothman, J. R. *Tetrahedron Lett.* In press.

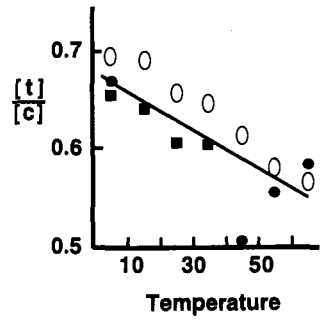

Figure 7. Temperature dependence of the [t]/[c] ratio for Ac-Hel$_1$-OH in D_2O. The three data symbols correspond to the three different regions for measurement of integration ratios (see Experimental Section). The line is calculated from the best fit values of $\Delta H°$ (−0.6 kcal/mol) and $\Delta S°$ (−2.9 eu).

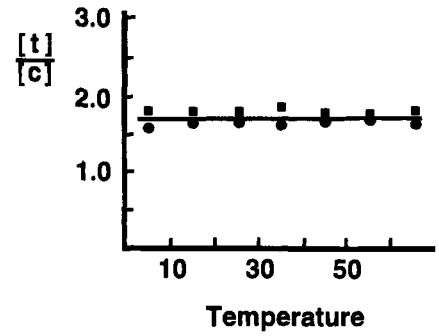

Figure 8. Temperature dependence of the [t]/[c] ratio for Ac-Hel$_1$-NHMe in D_2O. The two data symbols correspond to the two different regions for measurement of integration ratios (see Experimental Section).

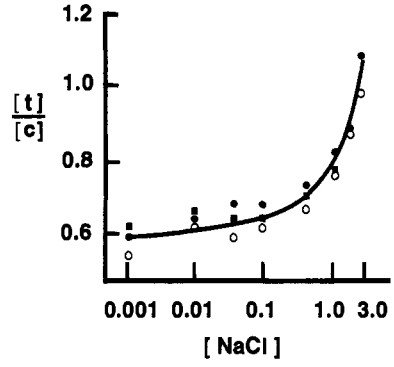

Figure 9. Variation with NaCl concentration of the [t]/[c] ratio for Ac-Hel$_1$-OH in D_2O. The three data symbols correspond to the three different regions for measurement of integration ratios (see Experimental Section).

the value expected for maximum alignment with the carbonyl lone pair but significantly different from the helical average of 147°.[22]

The dihedral angle betwen the two amide planes can deviate substantially from zero for well-defined hydrogen bonds found in proteins.[22] The out-of-plane dihedral angles (NC,OH) for te and ts states of Ac-Hel$_1$-NHMe are calculated as 132° and 130°, respectively. Clearly both te and ts state hydrogen bonds have substantial π character and share very similar angles. However, the O···H bond lengths calculated for te and ts states are significantly different. The intramolecular hydrogen bond formed by the ts state at 2.22 Å is more than 10% longer than that formed by the te state and significantly longer than the average value of 2.05 Å found for helices in proteins. This difference results from the tilt away from the helical axis that is induced in the C-2 pyrrolidine by the change in orientation of the sulfur. Consistent with this mechanism, the difference persists through modelings of a series of five Ac-Hel$_1$-A$_n$-NHMe and four Ac-Hel$_1$-L-Lac-A$_n$-NHMe conjugates; by calculation the te state always formed significantly shorter amide−amide hydrogen bonds. Badger's rule, which correlates bond length with bond force constant and strength, has been shown to apply to a wide variety of atomic interactions;[23] correlations of hydrogen bond length with strengths of donor acids and bases and therefore with hydrogen bond strength are also well-documented.[24] Thus the conclusion that can be drawn with greatest confidence from the MM studies is that the ts state most likely forms an intramolecular hydrogen bond that is significantly weaker than that formed by the te.

The Effects of Salt and Temperature on the [t]/[c] Ratio of Ac-Hel$_1$: Rates of t−c Equilibration

Isolated helices in aqueous solution are stabilized by high concentrations of NaCl, by the presence of alcohols such as trifluoroethanol (TFE), and by low solution temperatures.[11,12,25] The effects of temperature on the [t]/[c] ratios of Ac-Hel$_1$-OH and Ac-Hel$_1$-NHMe are shown in Figures 7 and 8.. The modest temperature dependences seen in Figure 7 indicate that the (t) state of Ac-Hel$_1$-OH is selectively disfavored by a temperature increase, although the effect is not large and corresponds to a $\Delta H°$ for (c) → (t) of −0.6 kcal/mol. The [t]/[c] ratio for the simple amide Ac-Hel$_1$-NHMe shows no detectable temperature dependence in the aqueous temperature range, and for this substance $\Delta H°$ must be substantially smaller. The effect of NaCl on the [t]/[c] ratio of Ac-Hel$_1$-OH is shown in Figure 9. The salt dependence is similar to that seen for helical peptides and proteins, and it probably reflects a local dielectric-induced selective stabilization of the (te) state with its three aligned amide dipoles.

In striking contrast to the behavior of peptides with a helical disposition which show a dramatic increase in the [t]/[c] ratio with an increase in TFE concentration, the [t]/[c] ratio of Ac-Hel$_1$-OH at 25 °C in TFE−water (0 to 40 mol % TFE) shows no systematic variation, with all data lying within a standard deviation of the mean and within the probable error of measurement ([t]/[c] = 0.59 (SD 0.04 for seven measurements)).

$$C \underset{k_{-1}}{\overset{k_1}{\rightleftharpoons}} T \qquad k_{obs} = (k_1 + k_{-1}) = k_1\frac{(K+1)}{K} \qquad (1)$$

where $K = k_1/k_{-1}$

For Ac-Hel$_1$-OH and its peptide derivatives changes of medium result in large changes in [t]/[c]. As noted previously,[26] the addition of TFE to water causes a dramatic increase in the [t]/[c] ratio of most peptide conjugates of Ac-Hel$_1$. Moreover, in the crystalline state the [t]/[c] ratio of Ac-Hel$_1$-OH differs markedly from that observed in water. As a result, by NMR-monitored kinetics experiments it is possible to measure the

(22) Baker, E. N.; Hubbard, R. E. *Prog. Biophys. Mol. Biol.* **1984**, *44*, 97−179. Jeffrey, G. A.; Saenger, W. *Hydrogen Bonding in Biological Structures*; Springer-Verlag: Berlin, 1991. Stickle, D. F.; Presta, L. G.; Dill, K. A.; Rose, G. D. *J. Mol. Biol.* **1992**, *226*, 1143−1159.

(23) Johnston, H. S. *Gas Phase Reaction Rate Theory*; The Ronald Press: New York, 1966; pp 72−77.

(24) Steiner, T. *J. Chem. Soc., Chem. Commun.* **1994**, 2341−2342.

(25) Kim, P. S.; Bierzynski, A.; Baldwin, R. L. *J. Mol. Biol.* **1982**, *162*, 187−199. Scholtz, J. M.; Marqusee, S.; Baldwin, R. L.; York, E. J.; Stewart, J. M.; Santoro, M.; Bolen, D. W. *Proc. Natl. Acad. Sci. U.S.A.* **1991**, *88*, 2854−2858.

(26) Kemp, D. S.; Boyd, J. G. *Peptides, Chemistry, Structure, Biology*; Rivier, J., Marshall, G., Eds.; ESCOM: Leiden, 1990; pp 677−679. Kemp, D. S.; Allen, T.; Oslick, S. L. *Peptides, Chemistry Structure, Biology*; Smith, J., Rivier, J., Eds.; ESCOM: Leiden, 1992; pp 353−355.

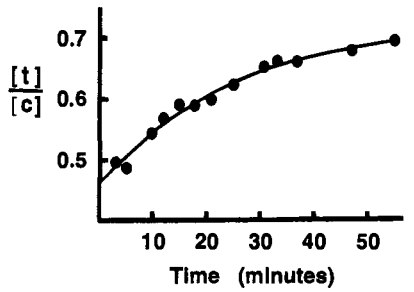

Figure 10. Kinetics of equilibration of the [t]/[c] ratio of Ac-Hel$_1$-OH in D_2O, 5 °C. The solid curve is calculated from [t]/[c] = [4.029 − exp(−0.045t)]/[5.587 + exp(−0.045t)], in which 0.045 min^{-1} = (k_{-1} + k_1), the first-order rate constant for the relaxation process. The dots correspond to data points. Data points are averages for two or three integration measurements.

rate of establishment of the (t)−(c) equilibrium in water following rapid solution or dilution. Figure 10 shows data obtained when crystalline Ac-Hel$_1$-OH is dissolved at 5 °C in D_2O and the [t]/[c] ratio is measured as a function of time. The equilibrium ratio is 0.68, which must equal a ratio of first-order forward and reverse rate constants k_1/k_{-1}, eq 1. Conversion of [t]/[c] to [t]/([c] + [t]) ratios, followed by a standard first-order rate analysis yields a value for (k_{-1} + k_1) of 0.045 min^{-1}, corresponding to a half time for the amide bond rotation of 15 min at 5 °C. From their known ratio and sum, k_1 is calculated as 0.026 min^{-1} and k_{-1} as 0.019 min^{-1}.

In 40 mol % trifluoroethanol the peptide conjugate Ac-Hel$_1$-Ala$_5$-OH is more than 95% (t) state conformer, but it changes to 65% (t) upon dilution to 2 mol % TFE. First-order rate analysis of time-dependent [t]/([t] + [c]) measurements of the rate of relaxation upon dilution at 10 °C gave (k_{-1} + k_1) of 0.07 min^{-1} with somewhat greater experimental uncertainty than that observed for the rate measurements with Ac-Hel$_1$-OH. This rate constant corresponds to a half time of 10 min and to k_1 and k_{-1} of 0.03 and 0.04 min^{-1}, respectively. The rate constants observed for these simple proline analogs are similar to those observed in water for the c−t interconversions of proline peptides and for proline residues in proteins.[27] In CD_3CN and $CDCl_3$ the c−t interconversions of Ac-Hel$_1$ derivatives proceed at much faster rates, in accord with the observations of Wolfenden et al. for Ac-Pro-NHMe in toluene.[28]

Relationship between the c−t and s−e Conformational Changes for Peptide Conjugates of Ac-Hel$_1$

The dilution experiment from high to low TFE concentration reported in the previous section for the peptide conjugate Ac-Hel$_1$-L-Ala$_5$-OH provides dramatic evidence for the conformational dynamics of the Ac-Hel$_1$ template. Prior to dilution, the ^{1}H spectrum in 40 mol % TFE−water shows (c)-state resonances that are barely detectable and (t)-state resonances that have largely (te) character. Immediately upon dilution the C-9ab and C-13ab proton resonances, which show the largest sensitivity to the s−e conformational change, assume δ and J values consistent with substantial acquired (ts) character. The (cs) resonances develop slowly, but the spectrum at equilibrium in 2−3 mol % TFE−water shows both a significant (cs) population as well as substantial (ts) character to the (t) state. These changes are only consistent with a selective, medium-dependent stability change of the (te) state, implying a simple quantitative

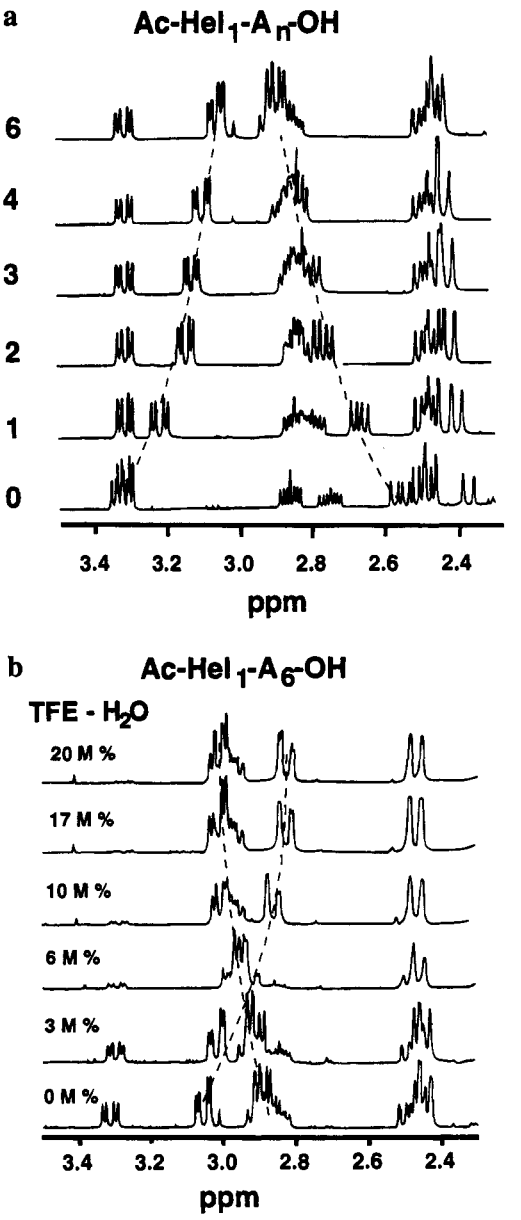

Figure 11. ^{1}H NMR spectra of Ac-Hel$_1$-peptide conjugates showing proton resonances at template sites C-9ab and C-13ab. The nearly invariant (cs) state resonances appear at C9b δ 3.32, C9a δ 2.50, C13b δ 2.85, C13a δ 2.42. The (t) state C-9 resonances shift substantially and are marked with dotted lines. (a) Spectra in water, 25 °C, showing the dependence of chemical shift and (t)−(c) relative peak intensity on the length of the alanine peptide. (b) Spectra in TFE−water mixtures, 25 °C, of Ac-Hel$_1$-A$_6$-OH, showing changes in (t)−(c) relative peak intensity and C-9ab chemical shifts with increasing [TFE].

correlation between [t]/[c] ratio and (ts)−(te) character. This feature of our model is tested here.

The changes in C-9 chemical shift and peak area are both dramatic and easily quantifiable. Peptide helices in water are stabilized both by an increase in length of the peptide chain and by medium changes such as the addition of TFE. Figure 11 shows a stacked plot of NMR chemical shifts in water of the C-9ab protons as the length of the peptide chain of Ac-Hel$_1$-Ala$_n$-OH is extended from n = 0 to 6. Addition of increasing amounts of TFE to an aqueous solution of Ac-Hel$_1$-Ala$_6$-OH results in further chemical shift changes in C-9a and C-9b t state resonances, accompanied by evident diminution of the resonances assigned to the c state, which undergo only a small change in chemical shift and none in coupling constant. NOE analysis of the (t) state spectrum of Ac-Hel$_1$-OH in water

(27) Brandts, J. F.; Halvorson, H. P.; Brennen, M. *Biochemistry* **1975**, *14*, 4953. Grathwohl, C.; Wuethrich, K. *Biopolymers* **1981**, *20*, 2623−2633.

(28) Radzicka, A.; Acheson, S. A.; Wolfenden, R. *Bioorg. Chem.* **1992**, *20*, 382−386.

reveals an interaction between protons at C-9b and C-12, characteristic of the (ts) state. By contrast, NOE analysis of the spectrum of Ac-Hel$_1$-L-Ala$_6$-OH in water or in TFE−water mixtures shows an interaction between protons at C-9a and C-13a, a diagnostic signature of the (te) state.[1]

In peak shape and coupling constants, the C-13 and C-9 regions of the ^{1}H spectra obtained at high TFE concentrations strongly resemble those observed in the structure-stabilizing solvent chloroform, and the (t) state chemical shift changes of Figure 11 are coordinated with changes in C-8,C-9 vicinal coupling constants.[1] The large range of conditions used in these studies and the limiting values observed for coupling constants, which at 2.5 and 9.9 Hz approach maximal and minimal values expected for vicinal coupling,[29] provide a suggestive but not compelling argument that the studies have in fact spanned the conformational space of the 8-ring lactam from essentially pure (ts) to pure (te).

Unfortunately, these limiting values alone cannot be used to argue that the limiting states are no longer state averages but correspond to single conformations. It is simple to demonstrate a two-state change but difficult to provide that it is complete. However, the correlation seen in Figure 11 between the experimentally measured [t]/[c] state ratio and the fractional (s−e) character of the (t) state implies that a very high state ratio must correspond to a (t) state with negligible s character. This unusual correlation of (t)−(c) relative abundances and (s)−(e) state average can be analyzed quantitatively to obtain a limiting value for the chemical shift of pure (te) state and to validate the qualitative conclusion that the phenomenological changes in NMR variables result solely from a selective stabilization of the (te) template conformation.

From the three-state model of Figure 1, eqs 2 and 3 can be

$$\delta_{obs} = \delta_{te}\frac{[te]}{[te]+[ts]} + \delta_{ts}\frac{[ts]}{[te]+[ts]}; \qquad \frac{[c]}{[t]} = \frac{[cs]}{[te]+[ts]}; \qquad K_1 \equiv \frac{[ts]}{[cs]} \quad (2)$$

$$\delta_{obs} = \delta_{te} + (\delta_{ts} - \delta_{te})K_1\frac{[c]}{[t]} = A + B\frac{[c]}{[t]} \quad (3)$$

derived, which predict a linear relationship between the experimental value of a C-9 chemical shift and the inverse of the [t]/[c] ratio. To test these equations, suitable corrections must be made for the effects of medium changes on chemical shifts, and linear behavior is only expected under the further significant assumptions that both the limiting chemical shift values and the [ts]/[cs] ratio are constants characteristic of the temperature and the solvent water, but not sensitive to the structure of the template−peptide conjugate or to small medium changes such as addition of TFE. An experimentally established linear relationship that exhibits context-independent constants A and B of eq 3 would thus validate all of these assumptions.

Abundant data are available from measurements in water and in TFE−water mixtures at 25 °C, and the results of Table 2 and Figure 12 include twelve different data sets comprising four significantly different structures at the template−peptide or template−amide junctions. These include correlations involving only changes in peptide length, as well as TFE−water titrations. A linear relationship between the C-9b chemical shift and the [c]/[t] ratio with an average correlation coefficient (CC) of at least 0.99 was observed for seven of these data sets, while five others gave CC values in the range of 0.82−0.98 with an average of 0.90. As seen in the table the intercepts and slopes obtained by linear regressions of different data sets are in satisfactory agreement throughout the twelve-member series, a striking result given the diversity of the structural series, and given that the length-dependent series in water present relatively small changes in the experimental variables, while TFE titrations present large changes. The line shown in the graphs of Figure 12 is calculated from the average slope and intercept for the seven high CC cases.

Table 2. Linear Regression Correlations between the H-9$_{1b}$ Chemical Shift and the [c]/[t] Ratio for Ac-Hel$_1$-Conjugates (25 °C)−$\delta_{1b} = A + B$[c]/[t]

conjugate	TFE (M %)	no. data points	A	B	CC
A.Water as a Solvent					
1. A_n-OH (n = 1 to 6)		6	2.910	0.289	0.988
2. A_n-OH (n = 2 to 6)		5	2.861	0.354	0.992
3. A_n-K-NH$_2$ (n = 2 to 5)		5	2.842	0.459	0.997
4. A_n-K-NH$_2$ (n = 2 to 5) and -A_5-X-NH$_2$ (X = Orn, Nle, R, dK)		9	2.851	0.428	0.898
B.TFE−Water Mixtures as Solvent					
5. A-OH	0−20	6	2.935	0.247	0.999
6. G-OH	0−20	6	2.914	0.299	0.996
7. NHMe	0−20	7	2.877	0.391	0.996
8. A_2-OH	0−8	4	2.891	0.310	0.998
9. A_4-OH	0−20	4	2.834	0.344	0.825
10. A_5-OH	0−20	4	2.851	0.381	0.998
11. A_6-OH	0−20	5	2.842	0.406	0.988
12. A_2GA_3-OH	0−20	5	2.890	0.314	0.933
13. A_2LA_3-OH	0−20	6	2.892	0.355	0.982
14. GGG-OH	0−20	5	2.933	0.345	0.997
15. Lac-A_2-OH	0−20	5	2.894	0.336	0.968
16. Lac-A_5-OH	0−20	4	2.900	0.459	0.990
		mean:	2.882 (0.03)	0.363 (0.06)	

The correlation of Figure 12a shows the effect of varying peptide length in water as a solvent, while Figure 12b shows the effect of TFE titration of three template−peptide conjugates. (In the latter graph the downward curvature evident for the data measured at small [c]/[t] values (i.e., at high [TFE]) may reflect uncertainties in the correction of observed chemical shift for the effect of TFE, as noted in the Experimental Section.) Figure 12c plots TFE titrations of monoamides. Strikingly, these are seen to obey the same correlation that is observed for medium-length peptides. This correlation therefore holds in cases for which changes in state ratio and fractional abundance result from addition of amino acid residues to a peptide site remote from the template junction, as well as in cases for which medium effects alter the stability of a single amide residue. Figure 12d shows data for a structural pair in which the template and a short alanine peptide are linked through a lactate ester spacer, preventing the conjugate from forming the first intramolecular hydrogen bond that almost certainly mediates the (t)−(c) structural change for the other structural classes reported in the table. Perhaps not coincidentally this pair exhibits the least satisfactory correlation of the study. The data show substantial scatter that undoubtedly reflects a significant structural reorganization at low TFE concentrations, yet δ_{9b} nevertheless is seen to vary with [c]/[t] in an approximately linear fashion, yielding a best slope and intercept similar to those observed for normal secondary amide-linked conjugates.

As noted above, the intercept term of the correlation must correspond to the limiting chemical shift value for H9b of the (te) state. The average value is found to be 2.87(0.04) for the cases restricted to CC > 0.99, and 2.89 for all cases. Its lack

(29) Jackman, L. M.; Sternhell, S. *Applications of Nuclear Magnetic Resonance Spectroscopy in Organic Chemistry*, 2nd ed.; Pergamon Press: Oxford, 1969; p 288. Abraham, R. J.; Fisher, J.; Loftus, P. *Introduction to NMR Spectroscopy*; Wiley-Interscience: Chichester, 1988; pp 44−45.

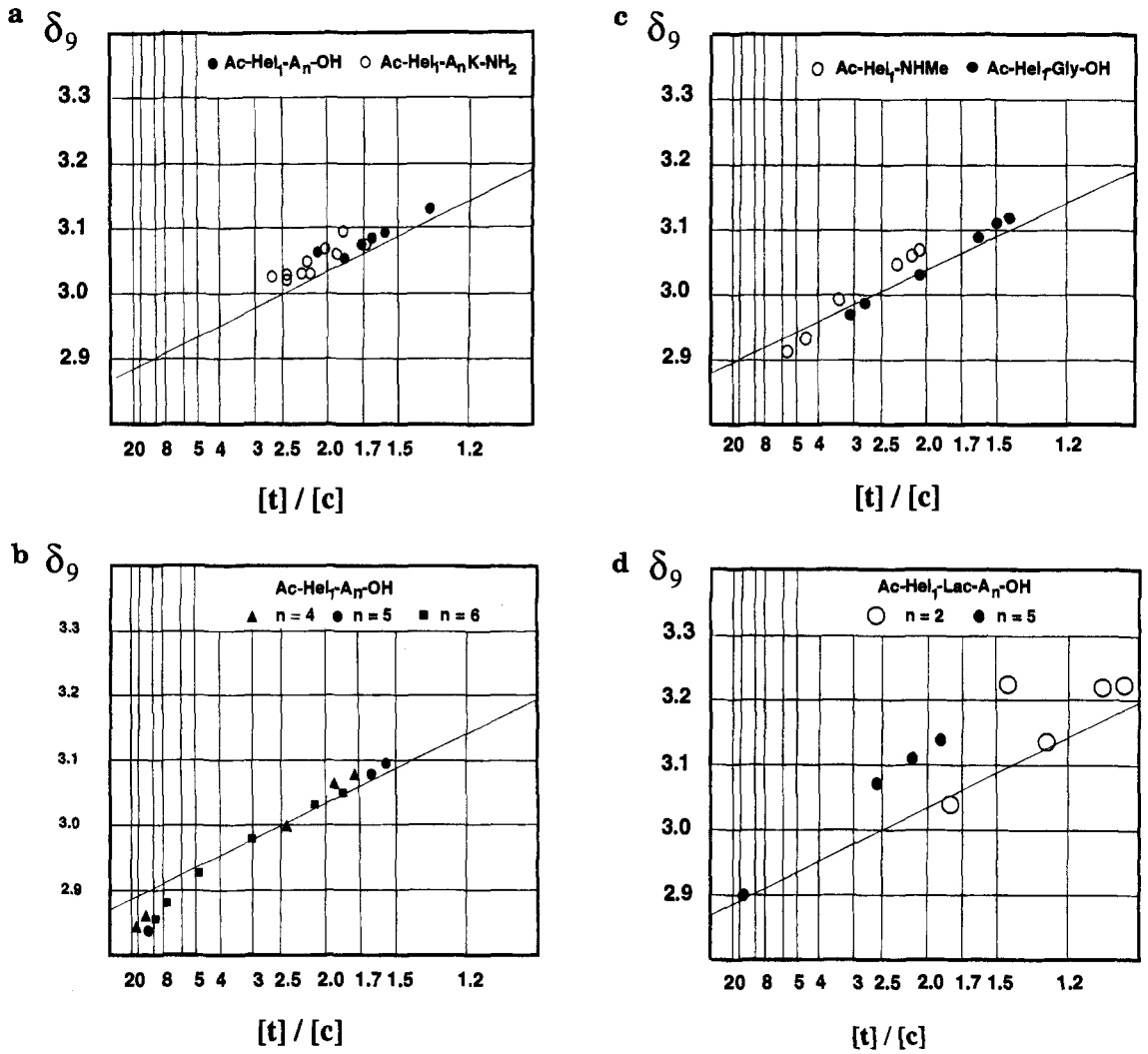

Figure 12. The experimental dependence of the ^{1}H NMR C-9b proton chemical shift on the [t]/[c] ratio: (a) data for Ac-Hel$_l$-A$_n$-OH (n = 4, 5, 6) and Ac-Hel$_l$-A$_n$-K-NH$_2$ (n = 2, 3, 4, 5) in water, 25 °C; (b) data for Ac-Hel$_l$-A$_n$-OH (n = 4, 5, 6) and Ac-Hel$_l$-A$_n$-K-NH$_2$ (n = 2, 3, 4, 5) in TFE–water mixtures, 25 °C; (c) data for Ac-Hel$_l$-G-OH and Ac-Hel$_l$-NHMe in TFE–water mixtures, 25 °C; and (d) data for Ac-Hel$_l$-L-Lac-A$_2$-OH and Ac-Hel$_l$-L-Lac-A$_5$-OH in TFE–water mixtures, 25 °C.

of dependence on structure at the peptide–template junction strongly supports the interpretation that the template behaves as a three-state switch that acts independently of the precise mechanism by which selective (te) stabilization is achieved. The slope term can be identified as a product of K_1 and the difference in limiting shift values for (ts) and (te) states and is also satisfactorily constant throughout the series studied. Since the (ts) state must be essentially unstructured at the peptide–template junction, it is expected to be modeled accurately by the value of δ 3.32 observed for (t) state resonances in derivatives that lack intramolecular hydrogen bonds, and as noted above, the (te) state δ is the linear constant A from (3). Accordingly K_1 can be calculated to be 0.79(0.14). Significantly, it is largely independent of peptide length or of (te) state stabilization through medium changes. This value for the [ts]/[cs] ratio can be compared with a value of 0.65 observed for Ac-Hel$_l$-OH in water at 25 °C (Figure 7) and with a value of 0.69 observed for Ac-Hel$_l$-Lac-OH, the unstructured lactate ester conjugate.

From the results of this section the three-state model for the conformational properties of Ac-Hel$_l$ conjugates is shown to be consistent with the available experimental data, and the constant K_1 of Figure 2, which defines the equilibrium between the nonnucleating (cs) and (ts) states, is shown to be invariant in water.

$$\text{fraction cs} = \frac{1}{(1 + [t]/[c])}; \quad \text{fraction ts} = \frac{K_1}{(1 + [t]/[c])};$$

$$\text{fraction te} = \frac{([t]/[c] - K_1)}{(1 + [t]/[c])} \quad (4)$$

$$\text{fraction nonnucleating} = \frac{(1 + K_1)}{(1 + [t]/[c])};$$

$$\text{fraction te} = \frac{([t]/[c] - K_1)}{(1 + [t]/[c])} \quad (5)$$

These results have two immediate consequences. First, as noted in (4), measurement of the [t]/[c] ratio defines the mole fractions of the three template conformational states. Second, since K_1 is invariant and links the non-nucleating (cs) and (ts) states, for many purposes these states can be paired and treated as a non-nucleating composite. The template conjugate in water can thus be characterized by a two-state equilibrium consisting of nucleating (te) and nonnucleating composite ((cs) + (ts)) template states in the respective abundances shown in (5).

Circular Dichroism Spectra of Ac-Hel$_l$-OMe and Ac-Hel$_l$-NHMe

The CD spectra of helical peptides in water provide a fingerprint for helical character, and an empirically derived linear

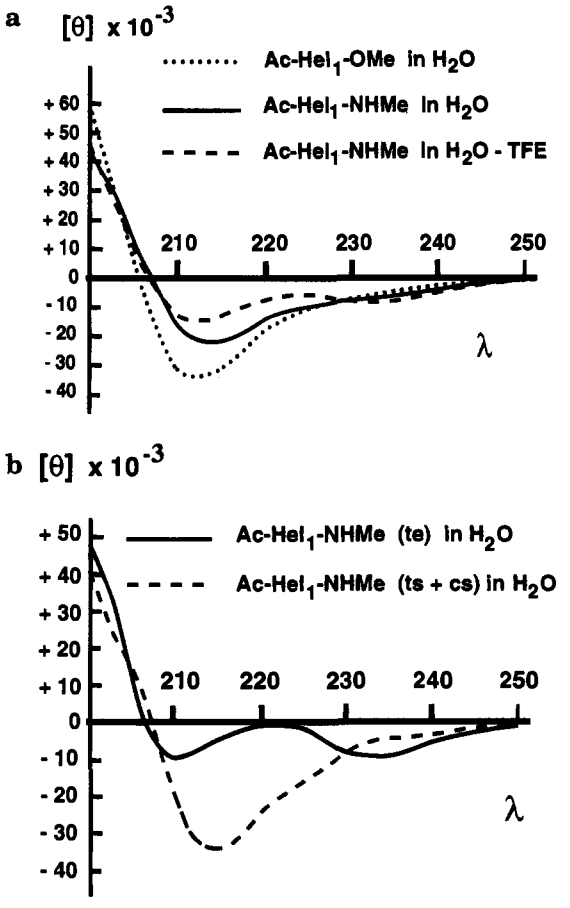

Figure 13. CD spectra of Ac-Hel$_1$-OMe and Ac-Hel$_1$-NHMe, 25 °C: (a) spectra in water, pH 7, and in 20 mol % TFE–water; (b) calculated spectra for the (te) and composite ((cs) + (ts)) states of Ac-Hel$_1$-NHMe in water, 25 °C (see text).

correlation with the magnitude at 222 nm of the molar ellipticity per residue provides the simplest and the most commonly used tool for quantitating fractional helicity.[30] For two reasons, an analysis of this type is unsuitable for monitoring helicity in short peptide conjugates of Ac-Hel$_1$. First, for short to medium-sized peptides, theory predicts a large length-dependence for molar residue ellipticity values.[31] Second, the three conformational states of Ac-Hel$_1$ exhibit strong CD absorption in the helical 200–250 nm range, attributable not only to the amide backbone but also to the thioether function. The CD spectra of Ac-Hel$_1$-OMe in water and Ac-Hel$_1$-NHMe in water and in 20 mol % TFE–water are shown in Figure 13a. The CD spectrum of the ester is nearly invariant to added TFE, consistent with the invariant [t]/[c] ratio observed for the corresponding acid. The [t]/[c] ratio of the amide increases from 1.7 in water to 5.3 in 20 mol % TFE–water, corresponding to a change in mole fraction of (te) state from 0.36 to 0.72, and Figure 13a shows that a significant change in the CD spectrum results. If the observed amide spectra are mole fraction weighted sums of two limiting TFE-invariant spectra for the (te) state and the composite ((cs) + (ts)) state, then a simple linear deconvolution yields these limiting spectra, with greater calculated precision for the former. These deconvolutions are shown in Figure 13b. A measure of the validity of the assumption underlying the deconvolution is the near identity of the composite ((ts) + (cs)) spectrum of Figure 13b and the observed spectrum for Ac-Hel$_1$-OMe shown in Figure 13a. Significantly, the calculated CD ellipticity of the (te) state shows a long wavelength minimum at 233 nm and is nearly zero at 222 nm. These deconvoluted spectra provide the starting point for development of an algorithm for calculating helicity from CD spectra of Ac-Hel$_1$-peptide conjugates.

(30) Chang, C. T.; Wu, C.-S. C.; Yang, J. T. *Anal. Biochem.* **1978**, *91*, 13–31. Woody, R. W. *The Peptides*; Volume I, Academic Press: New York, 1985; Vol. 1, pp 15–114.
(31) Manning, M. C.; Woody, R. W. *Biopolymers* **1991**, *31*, 569–586.

Discussion

Two fundamental questions remain to be addressed—what is the evidence that the nonnucleating (cs) state of a peptide Ac-Hel$_1$ conjugate can be used as an energetic reference for judging the selective stabilization of the (te) state, and what structural factors underlie the interaction of the Ac-Hel$_1$ template with a linked peptide? Answers to the first question define the scope of application of the reporter functions of Ac-Hel$_1$. Answers to the second question define the nature of the templating principle, its limiting magnitude, and its potential for generalization.

The causal relationship between the [t]/[c] ratio and the energetics of template–peptide interactions underlies answers to both questions and provides a convenient starting point for the subsequent discussion. From Figure 12, it is clear that even a simple Ac-Hel$_1$- conjugate such as Ac-Hel$_1$-NHMe, which can form only a single intramolecular hydrogen bond, is dramatically sensitive to medium changes such as addition of TFE, which selectively stabilizes the (te) state. For a derivative that can form only one hydrogen bond, the mass action expression ([ts] + [te])/[cs] can be redefined rigorously in terms of substates of (te) as in (6). The (te$_0$) state is the substate of (te) that is present in the absence of any selective stabilization by a linked peptide, for example, in aqueous solutions of derivatives such as Ac-Hel$_1$-OMe or Ac-Hel$_1$-OH. Attempts to define the [te$_0$]/[ts] or [ce$_0$]/[cs] ratios experimentally have thus far failed, but likely estimates lie in the range of 0.05–0.2. The (te$_1$) state is defined as containing a single hydrogen bond at the template–peptide junction between the acetamido carbonyl of the template and the first amide NH of the conjugate. The equilibrium constant linking this state to (te$_0$) must be significantly larger than unity so that the two (te) micro-state steps (ts) → (te$_0$) → (te$_1$) result in a significant change in [t]/[c], as observed experimentally for derivatives like Ac-Hel$_1$-NHMe.

The observations that helix initiation by Ac-Hel$_1$ is blocked by a sarcosine (*N*-methylglycine) substitution at the template–peptide interface[1] and markedly impeded by a lactate substitution implies that formation of a stable hydrogen bonded (te$_1$) state is a strong precondition for further structure initiation in a longer peptide conjugate. By a generalization of the above reasoning, the expression linking the [t]/[c] ratio monitored at the template with the equilibrium constant X for structure initiated by the (te) conformation of the template must be a simple linear function, eq 7, in which the additive constant K_1 reflects the [t]/[c] ratio of the template in the presence of local interactions at the peptide–template interface for (cs), (ts), and (te$_0$) states but in the absence of any stabilizing (te$_i$) interactions, and the multiplicative constant K_2 reflects the efficiency of the template initiation process.

$$\frac{[t]}{[c]} = \frac{[ts] + [te_0] + [te_1]}{[cs]} = K'_1\left(1 + \frac{[te_0]}{[ts]}\left(1 + \frac{[te_1]}{[te_0]}\right)\right) = K_1 + K_2 \quad (6)$$

where [te] = ([te$_0$] + [te$_1$]); K'_1 = [ts]/[cs]; $K_1 = K'_1(1 + [te_0]/$

[ts]); $K_2 = K'_1([te_0]/[ts])([te_1]/[te_0]) = [te_1]/[cs]$.

$$[t]/[c] = K_1 + K_2X \tag{7}$$

In subsequent studies we propose to use the measured concentration ratio [t]/[c] of peptide conjugates of Ac-Hel$_1$ to quantitate the stability of helices initiated in the peptide sequence. As Lesk has cautioned,[7] before the [t]/[c] data can be used, the (cs) state, which is the energetic reference, must be shown to be free of length-dependent structure. In effect, under the given experimental conditions the (cs) state must provide a valid energetic representation of a randomly structured peptide. A necessary but not sufficient argument draws on the absence of detectable peptide–peptide or peptide–template NOE interactions in the (cs) state in a variety of solvents for all peptide conjugates of Ac-Hel$_1$ that have been examined.[1] More general arguments follow from the observation noted above that K_1 is invariant to a wide range of structural changes. Since the analysis of eq 3 can be viewed as weighing the stability of the (cs) state relative to that of the (ts), the experimental invariance of K_1 implies that any selective stabilization that might occur in the (cs) state must be quantitatively mirrored in comparable stabilization found in the (ts) state. Length-dependent (cs)-stabilizing structure, if present, might be expected to reveal itself to NMR scrutiny under the high TFE concentrations used in some examples of the study, but no evidence for it has been observed. The simplest interpretation of the experimental invariance of K_1 is that neither (ts) nor (cs) states contain significant length-dependent structure for any of the examples studied.

$$\frac{[t]}{[c]} = \frac{[ts](1 + F(x)) + [te]F(x)}{[cs](1 + F(x))} = K_1 + K_2\frac{F(x)}{(1 + F(x))} \tag{8}$$

$$\frac{[t]}{[c]} = \frac{[ts](1 + \alpha F(x)) + [te]F(x)}{[cs](1 + \alpha F(x))} = K_1 + K_2\frac{F(x)}{(1 + \alpha F(x))} \tag{9}$$

A more compelling case can be made. Algebraic models can be devised in which both (cs) and (ts) states initiate equivalently stabilizing conformations in a linked peptide, meeting the condition of K_1 invariance. However, for selected medium-sized peptide conjugates of Ac-Hel$_1$ in aqueous TFE mixtures, [t]/[c] ratios can be found to exceed 50.[32] This result is inconsistent with many such models and severely constrains the remainder. For example, in expression 8 the proposed length-dependent component of stabilization of (cs) is represented by an arbitrary nonnegative function $F(x)$, which for a peptide of sufficient length almost certainly must have the same form for all template states. Equation 8 can yield [t]/[c] ratios no larger than $(K_1 + K_2)$, and since K_1 and K_2 by measurement are fixed and small, the equation is inconsistent with large [t]/[c] ratios. An alternative model is given by (9) in which the function $F(x)$ of (8) is altered to include a factor α reflecting the extra inefficiency of starting structure from template (cs) and (ts) states. If [t]/[c] = 50, with experimental values of $K_1 = 0.7$ and $K_2 = 0.2$, α must meet the condition that $246/F(x) = (1 - 246\alpha)$; since α and $F(x)$ must be positive, α can be no larger than 0.004, which is an insignificant correction to the stability of the cs state.

The remaining case to be considered postulates a small correction to the stability of both (cs) and (ts) that is not length dependent but occurs locally as a result of interactions close to the template region. This possibility points up the difficulty of defining the stage at which the template–helix interface ends and true helix begins. Previously we have noted that a major virtue of an expanded version of the linear mass action expression 7 is retention of its overall functional form if the peptide–template junction is defined to be more inclusive and the site of helix initiation is redefined to occur further along the peptide chain.[1] Energetic anomalies that may occur within the first few peptide residues can thus be subsumed within redefined constants K_1 and K_2 that characterize the template–peptide interface. A detailed analysis of this case is provided in the third paper of this series.

(32) Kemp, D. S.; Groebke, K. Unpublished observations.

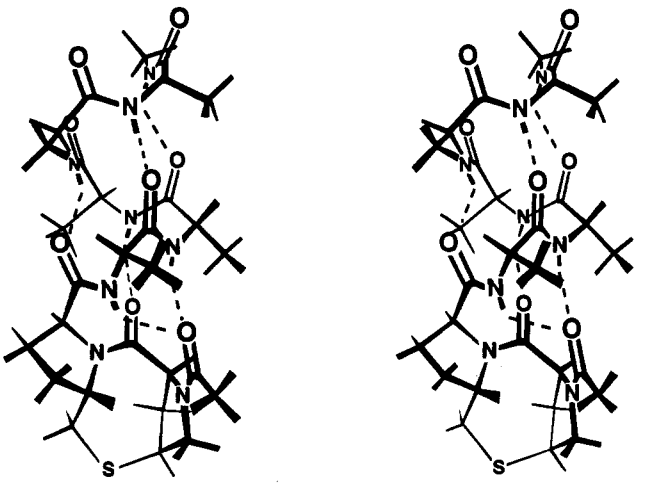

Figure 14. Computer-generated stereodiagram of the MM-minimized (vacuum) helical (te) conformation of Ac-Hel$_1$-A$_5$-NHMe, showing hydrogen bond geometry at the template–peptide junction.

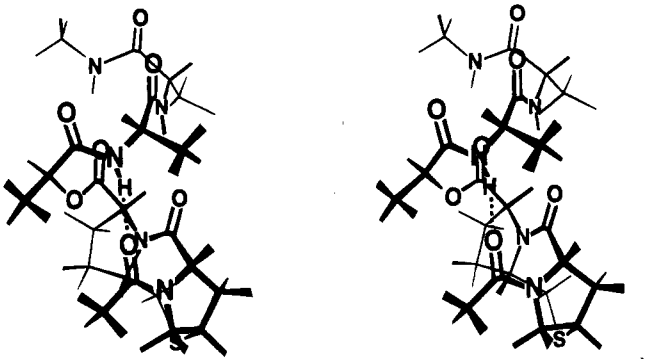

Figure 15. Computer-generated stereodiagram of the MM minimized (vacuum) helical (te) conformation of Ac-Hel$_1$-L-Lac–A$_2$-NHMe, showing hydrogen bond geometry at the template–peptide junction.

We conclude that with due precautions, the (cs) state of the RCT Ac-Hel$_1$ does indeed provide a satisfactory energetic model for the linked peptide in an unstructured state under a wide range of experimental conditions in aqueous solution. The experimental [t]/[c] ratio must therefore be a linear function of helical stability of the peptide in the (te) state, relative to the unstructured (cs) state peptide.

Since X-ray structural data are not yet available for helical conjugates of Ac-Hel$_1$, a causal understanding of Ac-Hel$_1$ as a helix initiator must begin with the MM-generated structure shown in the stereodiagram of Figure 14. In regarding this structure, Ac-Hel$_1$ can be viewed as a constrained analog of the N-blocked dipeptide *N*-acetyl-L-prolyl-L-proline, and indeed it contains only two additional atoms. However, N-Ac-Pro-Pro is unlikely to share helix-initiating features with Ac-Hel$_1$ since van der Waals interactions between its pyrrolidine rings prevent it from assuming any significant fraction of the conformation present in Ac-Hel$_1$. This compact conformation defines a confluent hydrophobic region spanning the hydrocarbon functions of the pyrrolidine rings and including a small

pocket created by the added sulfur of the thiomethylene function. As is evident from Figure 14, the first intramolecular hydrogen bond of an amide conjugate of Ac-Hel$_1$ must form within this pocket.

Ac-Hel$_1$ is deficient as an α-helical template in that it lacks one intramolecular hydrogen bonding site. The formal possibility exists that the amide NH at the template junction of Ac-Hel$_1$ might forgo intramolecular hydrogen bond formation, resulting in initiation of a structurally perfect α-helix in a linked peptide. The properties of derivatives that cannot form this hydrogen bond exclude this possibility. Comparison of the pair of conjugates Ac-Hel$_1$-Ala$_3$-OH and Ac-Hel$_1$-L-Lac-Ala$_2$-OH (Lac = lactate ester) shows that the ester has a dramatically reduced capacity to selectively stabilize the (te) state of the template. Nor is it surprising that this should be the case. The torsional ψ angle of the first peptide amide at the template junction of the (te) state is constrained to two narrow energy minima (Figure 5), the lower of which places it in the highly hydrophobic environment of the template where water molecules, if available, are likely to differ in hydrogen bonding capacity from bulk water. Thus for two reasons, the $\Delta G°$ for intramolecular hydrogen bond formation at this site is expected to be unusually favorable: first, the effective molarity of competing water in this region is likely to be low, and second, the effective molarity of the hydrogen bonding site of the acetamido residue is likely to be unusually high. Evidence for the unusual strength of this intramolecular hydrogen bond is available from the magnitude of [t]/[c] in pure water for monoamide conjugates as well as their large increase upon TFE titration. This hydrogen bond is structurally of the 3_{10} helical type, but MM modeling of the conformations of these conjugates suggests that a bifurcated hydrogen bonding structure shown in Figure 14 permits the induced helix to relax into a good approximation of an α-helical conformation within two residues. Theoretical calculations,[33] X-ray structural data of Karle,[34] and recent ESR-derived distance measurements of Millhauser[35] are all consistent with a rapid dynamic equilibrium between 3_{10} and α structures for short unaggregated helical peptides in water. We have independently observed that a triproline-derived N-terminal RCT initiates a polyalanine-based 3_{10} helix that relaxes into a structure that is largely α within one helical loop.[21]

The lactate derivative Ac-Hel$_1$-L-Lac-L-Ala$_5$-OH cannot form the first hydrogen bond to the template acetamido carbonyl, but it is able to form a second, which is explicitly shown in the stereodiagram of Figure 15. The reporter features of the template thus appear to reflect the relative strengths of two intramolecular hydrogen bonds formed between the carbonyl oxygen of the acetamido function of the template and the successive amide NH functions at the first two sites of the peptide chain. The formation of either of these results in a selective stabilization of the (te) state, although for reasons discussed above, the stabilizing effect of the H-bond to the first amide NH is significantly greater.

The (ts) to (te) switching effect that is quantitatively correlated with a change in [t]/[c] ratio poses a major structural riddle that has clear relevance to current debates concerning the energetics of intramolecular hydrogen bond formation. The likely explanation for this effect is that (te) states form stronger intramolecular hydrogen bonds from the acetamido carbonyl oxygen and peptide amide NH functions at sites 1 and 2. At present the evidence for the greater strength of (te) over (ts) hydrogen bonds rests on the significantly greater length observed consistently in pairs of structures generated by molecular modeling. Ac-Hel$_1$ appears to be unique in demonstrating an emphatic two-state selectivity between a pair of hydrogen-bonded structures that differ as subtly as the ts and te states. The emphatic preference of (te) over (ts) corresponds to an energy difference of hydrogen-bonded states of 0.6 to 1 kcal/mol and must reflect a fundamental property of amide−amide hydrogen bonds. We are exploring confirmation by X-ray diffraction analysis of our conclusion that this property may be attributed to the length of the hydrogen bond.

Although the evidence at this point is only suggestive, the local hydrophobicity at the site of helix initiation may also contribute significantly to the helix-initiating capacity of the templates we have thus far studied. Replacement of the Ac-Hel$_1$ acetyl by a bulky pivaloyl group results in a dramatic increase of both the [t]/[c] ratio and the e-character of the (t) state. A conformationally constrained triproline template that contains all of the atoms of Ac-Hel$_1$ within its structural framework but which has a greatly augmented local hydrophobicity exhibits high helical initiating capacity that is largely independent of solvent.[21] This interpretation stresses the role of local solvation in determining the energetics of hydrogen bonds that stabilize secondary structure, a point that has been recently discussed by Englander.[36]

Summary

The primary reporter property of the RCT Ac-Hel$_1$- is the magnitude of the [t]/[c] ratio, which can be easily measured as a ratio of integrated intensities of ^{1}H NMR resonances. This ratio is a simple function of the template-induced stabilization of the (te) state of Figure 2 by the linked polypeptide. The (cs) and (ts) states have been shown to lack state-specific length-dependent stabilization by the linked polypeptide, rendering this RCT an accurate probe of the (te) state stability, relative to that of the random coil. Measurement of the [t]/[c] ratio has been shown to define the mole fractions of the three template states: (cs), (ts), and (te).

For aqueous solutions, the rate constants for the (c)−(t) state interconversion have been measured, along with the sensitivity of the [t]/[c] ratio to changes in temperature, salt concentration, and concentration of the helix-stabilizing alcohol trifluoroethanol. The CD spectra of the Ac-Hel$_1$ (te) state and the composite ((cs) + (ts)) state have been obtained by a deconvolution analysis.

The substate structure for the three major conformations of Ac-Hel$_1$ as esters and amides has been examined by molecular mechanics analysis, and it is argued that for Ac-Hel$_1$ amides, a difference in the lengths of intramolecular hydrogen bonds between the amide NH and the acetamido carbonyl oxygen is the likely origin of the selective stabilization of the intrinsically less abundant (te) state over the more abundant (ts) state. The results of this discussion, taken with those of the subsequent papers in this series, provide a rigorous foundation for the application of Ac-Hel$_1$ as a versatile and sensitive reporter of the energetics of helix stabilization in water and in other solvents.

(33) Marshall, G. R.; Bensen, D. D.; Clark, J. D.; Hodgkin, E. E.; Zabrocki, J.; Leplawy, M. T. *Peptides—Chemistry, Structure, Biology*; Rivier, J. E., Marshall, G., Eds.; ESCOM: Leiden, 1990; pp 873−876. Huston, S. E.; Marshall, G. R. *Biopolymers* **1994**, *34*, 75−90.

(34) Karle, I. L.; Flippen-Anderson, J.; Sukumar, M.; Balaram, P. *Proc. Natl. Acad. Sci. U.S.A.* **1987**, *84*, 5087−5081. Karle, I. L. *Biopolymers* **1989**, *28*, 1−14.

(35) Todd, A. P.; Millhauser, G. L. *Biochemistry* **1991**, *30*, 5515−5523. Fiori, W. R.; Miick, S. M.; Millhauser, G. L. *Biochemistry* **1993**, *32*, 11957−11962.

(36) Bai, Y. W.; Milne, J. S.; Mayne, L.; Englander, S. W. *Proteins, Structure, Function, Genetics* **1993**, *17*, 75−86.

(37) Roberts, J. D. *An Introduction to the Analysis of Spin−Spin Splitting in High Resolution Nuclear Magnetic Resonance Spectra*; W. A. Benjamin: New York, 1961.

Experimental Section

Abbreviations: SPPS, solid phase peptide synthesis; HOBT, 1-hydroxybenzotriazole; DIEA, diisopropylethylamine; DCM, dichloromethane; DMF, *N,N*-dimethylformamide; DIC, diisopropylcarbodiimide; PFP ester, pentafluorophenyl ester; TFA, trifluoroacetic acid; 4-DMAP, 4-(dimethylamino)pyridine.

Instrumentation. Varian VX500S and 501S spectrometers (500 MHz) were used for ^{1}H NMR spectroscopy, and FIDs were processed on Sun Microsystems Sparc 2 workstations using the Varian Instruments VNMR 3.1 software. Chemical shifts are reported in ppm (δ) downfield from (trimethylsilyl)propionic-2,2,3,3-d_4 acid (TMSPA) for aqueous solutions and from tetramethylsilane (TMS) for organic solutions. Splitting patterns are designated as follows: s, singlet; d, doublet; t, triplet; q, quartet; dd, doublet of doublets; m, unresolved multiplet; br, broad. Analytical thin-layer chromatography (TLC) was carried out on aluminum-backed precoated silica gel 60 F-254 plates (Merck). Analytical high-performance liquid chromatography (HPLC) was performed on a Waters system consisting of two 501 pumps, a U6K injector, a model 660 automated gradient controller, a model 730 data module, a model 490 programmable multi-wavelength detector, and a Vydec 0.46 × 25 cm (218TP54) C_{18} reverse-phase column. Elution was carried out at 1.0 mL/min using both isocratic and linear/nonlinear gradients. Preparative scale HPLC was carried out on a Waters system composed of a model 590 pump fitted with preparative heads, an Autochrome DPG/S pre-pump solvent mixer, a Rheodyne injector, a model 484 variable-wavelength detector, and either a Baker 5.03 × 25 cm C_{18} (RP-7297-47) or a Vydec 2.2 × 25 cm C_{18} (218TP1022) preparative scale column. Elution was carried out at 18 mL/min for the Vydec column and at 80 mL/min for the Baker column.

CD spectroscopy was carried out in 1-mm strain-free quartz cells using an Aviv model 62 DS circular dichroism spectrometer. For ease in preparation, all samples were carefully dried in vacuum, weighed, and dissolved in a known amount of CH_3CN to form a stock solution, aliquots of which were carefully diluted into the solvent of interest prior to data collection. After dilution, the Ac-Hel$_1$-OMe sample solutions were 99.8% by volume in the solvent of interest, and the Ac-Hel$_1$-NHMe solutions were 99% by volume in the solvent of interest. CD spectra in water of solutions prepared in this manner from crystalline Ac-Hel$_1$-OH and noncrystalline Ac-Hel$_1$-OMe (oil) were superimposable and showed indistinguishable ellipticities.

Low-resolution mass spectra of template conjugates over 500 AMU were measured using plasma desorption on an Applied Biosystems Bio-Ion 20 instrument. Mass spectra on substances below 500 AMU were carried out by electron impact (EI-MS) on a Finnegan MAT 8200 instrument using either a glycerol/methanol matrix or a nitrobenzyl alcohol/methanol matrix. High-resolution mass spectra were obtained by fast atom bombardment (FAB-MS) on a Finnegan MAT 8200 spectrometer using a glycerol/methanol matrix.

Sample Preparation for NMR Spectroscopy. For studies carried out in D_2O the Ac-Hel$_1$-peptide conjugate was twice dissolved and evaporated in vacuum from 99.9% D_2O, lyophilized from 99.96% D_2O, and dried under high vacuum overnight. Most spectroscopic solutions were prepared in 99.96% D_2O, treated with 0.1% CF_3CO_2D, and examined in a 5-mm probe at a sample volume of 700−750 μL to optimize sample field homogeneity. TFA was not added to Ac-Hel$_1$-NHMe solutions. The effective pD of these solutions was 0.6−1.1. For most peptide conjugates a sample concentration in the range of 3−20 mM was studied. Selected samples, particularly involving higher molecular weight conjugates within a series, were checked for evidence of aggregation by orders of magnitude dilution. In all reported cases dilution resulted in no significant changes in chemical shift or peak width. Temperatures of all routine NMR measurements were maintained at 25−27 °C (3−4 °C above ambient) to minimize temperature fluctuations. TFE−water mixtures were made up to the appropriate mole percentage of components and were ca. 0.25 M in TFA; no change in the NMR properties of Ac-Hel$_1$-AALAAA-OH was seen in solutions containing 0.18 to 1.81 M TFA.

Corrections and Data Analysis for the Correlations of Table 2 and Figure 12. Chemical shifts for C9b protons were obtained as an average of the chemical shifts of the quartet of resonances; the error between this value and that calculated by a rigorous analysis[37] is small. Chemical shift values were not included in the study for cases in which peak overlap with C9a and C13b protons is observed (see Figure 11b). Chemical shift values measured in TFE−water mixtures were corrected for the effect of solvent change. An estimate of the magnitude of this change was made in two ways. For Ac-Hel$_1$-A$_6$-OH at TFE concentrations greater than 20 mol %, the observed chemical shift change is essentially entirely attributable to change in solvation. The chemical shifts of the (t) state C9a and C9b proton resonances were linearly correlated with [TFE] in the range of 20−40 mol %; a mean of the slope of these correlations was found to be −0.0025. Alternatively, the (c) state C9b proton resonances for Ac-Hel$_1$-L-Lac-OH and Ac-Hel$_1$-OH which show no change in [t]/[c] with TFE, and those for Ac-Hel$_1$-A-OH, Ac-Hel$_1$-A$_2$-OH, and Ac-Hel$_1$-A$_2$-G-A$_3$-OH, which show only a modest change in [t]/[c] with TFE, were each linearly correlated with [TFE] over the range of 0 to 20 mol %, yielding an average slope of −0.0022. This value was used to correct all data measurements for studies in TFE−water mixtures.

Although the SD within a single correlation was in the range of 0.01, the SD for the mean of five series was ±0.00064. Variations in the TFE correction significantly change the constant B of Table 2 for correlations based on Ac-Hel$_1$-A$_n$-OH ($n > 3$), for which δ_{9b} values at very small [c]/[t] ratios strongly determine the slope. Data of these types are found in Figure 12b. Thus for Ac-Hel$_1$-A$_6$-OH, a TFE correction of (−0.0022 + 0.00064) gives $A = 2.832$ and $B = 0.425$, and a correction of (−0.0022 − 0.00064) gives $A = 2.850$ and $B = 0.340$. This is the maximum uncertainty in B values expected from errors in the TFE correction term; uncertainties clearly lie within the range seen for the series correlations of Table 2.

Temperature-Dependent NMR Spectra. Variable-temperature NMR studies were carried out in the range of 5−65 °C using a Variant VTC4 temperature control apparatus. After a temperature change the probe and sample were equilibrated for 10 min before shimming, then measurements were made. Calibration was carried out with a methanol standard.

Integration of ^{1}H NMR Resonances and Calculation of [t]/[c] Ratios. Although some measurements were made for a few derivatives (Ac-Hel$_1$-A$_n$-OH ($n = 1-5$); Ac-Hel$_1$-G$_n$-OH ($n = 3$); Ac-Hel$_1$-L-Lac-A$_n$-OH ($n = 2, 5$)) in H_2O/D_2O using presaturation of the HDO peak, all other measurements were conducted in high-purity D_2O with precautions to exclude HDO, avoiding the need for water suppression and resulting in an improvement in precision and accuracy of peak integration. Care was taken to ensure maximum accuracy.[38] Experiments were run at concentrations of 3−20 mM and usually consisted of 256 or 512 transients. Long acquisition times (3−4 × T_1) were usually employed to enhance resolution and ensure complete relaxation of nuclei. Spectral widths were usually 8000 Hz, and the one-dimensional FIDs were digitized with 32 000 points, resulting in a resolution of 0.25 Hz/point. All spectra were carefully phased to pure absorption, and a linear base line correction routine (lvl/tlt) was applied to each region of the spectrum in which integrations were measured. As is apparent from Figure 11a,b, spectra of Ac-Hel$_1$-peptide conjugates in water and in water−TFE mixtures differ markedly in the degree of peak overlap in the 2.4−3.4-ppm region and elsewhere in the spectrum. The following protocol serves to illustrate the general approach. For many cases the spectrum was divided into three regions for integration purposes—(1) 3.70−4.15 ppm, comprising the (c) and (t) resonances for C12a, C12b, and C11 protons. In this region, the nonoverlapping (c)-state C11 resonance was used to estimate the relative abundance of the (c) state. (2) 2.70−3.40 ppm, comprising the C9bc, C9bt, C9at, C13bt, and C13bc proton resonances together with proton resonances of a lysine side chain, if present. In all derivatives without exception, the unobscured C9bc proton resonance was used to estimate the relative abundance of the (c) state. (3) 2.05−2.6 ppm, comprising the C9ac, C13ac, C13at, the (c) and (t) resonances of two protons at C6,C7, and the (c) and (t) resonances of the acetyl methyl. Region 3 was only used if the proton resonances for the acetyl methyl were free of overlapping peaks. Integrations in general were measured 8 Hz outside of the outermost resonance of each multiplet, but in cases in which spectral overlap was observed, the entire region was integrated, and

(38) Derome, A. E. *Modern NMR Techniques for Chemistry Research*; Pergamon Press, Inc.: New York, 1987; pp 168−172.

suitable corrections were applied. For spectra measured in HOD, the proximity of the suppressed water peak to region 1 resonances led to substantial distortions, and integration in regions 2 and 3 was used exclusively in these cases. Spectra measured in TFE−D_2O mixtures showed large solvent shifts in region 3, and integration in regions 1 and 2 was used exclusively.

The (c) state resonance is almost invariably the minor and the (t) state the major resonance; the analysis is thus unusually sensitive to (c) state integration errors. The accuracy of integration estimates of [t]/[c] thus depends on the availability of the unincumbered, integrable (c)-state resonance, together with a block of nondifferentiated (t)- and (c)-state resonances. The unnormalized (t)-state integration was calculated as the overall integrated intensity of the undifferentiated block (which includes its component of n (c)-state resonances), less n times the integrated intensity of the isolated (c)-state resonance, all divided by the number of (t)-state protons represented in the undifferentiated block.

From studies of derivatives prepared for the host−guest series Ac-Hel_1-AAXAAAAK-NH_2, 56 examples of calculations of [t]/[c] ratios were available for statistical analysis. The [t]/[c] ratios ranged from 2.0 to 3.6, and the standard deviations for integration ratios calculated in the three spectral regions described above ranged from 0.00 to 0.34. The standard deviations themselves showed a mean of 0.11 and a standard deviation of 0.07. In general, calculations from integration in region 1 appear to slightly underestimate [t]/[c], and those from region 3 result in a slight overestimation.

Molecular Modeling. Molecular modeling was carried out using the CHARMm QUANTA@3.3 software of Molecular Dynamics Inc., following the previously described procedures.[1] Simulations were in vacuum, and minimizations were carried out with a final 15 cycles of the Newton−Raphson algorithm to ensure convergence. The torsional scans of Figure 5 were carried out with each torsional angle fixed and with 500 cycles of adopted-basis Newton−Raphson minimization.

Synthesis of Ac-Hel_1-Peptide Conjugates. The syntheses of Ac-Hel_1-OH and its polyAla conjugates Ac-Hel_1-A_n-OH (n = 1 to 6) were carried out as described previously.[1] All peptide conjugates that terminate in a primary amide function were synthesized by solid phase peptide synthesis using the protocol described below, purified by preparative HPLC and characterized by ^{1}H NMR and plasma desorption MS. Other derivatives were synthesized by solution phase synthesis.

Ac-Hel_1-NHMe. To a chilled solution of Ac-Hel_1-OH (3.7 mg, 12 μmol), methylamine hydrochloride (1.1 mg, 16.3 μmol), and HOBt (2.5 mg, 16 μM) in DMF (300 μL) were added DIEA (2.8 μL, 16 μmol) and 1-(3-(dimethylamino)propyl)-3-ethylcarbodiimide hydrochloride (3.7 mg, 19 μmol). After 1 h at 0 °C and 1 day at 25 °C the solution was evaporated, and the residue was taken up in MeCN/H_2O and purified by preparative HPLC (0→40% MeCN(H_2O with 0.1% TFA/linear gradient)/20 min, RT 7.3 min). Evaporation of the appropriate fractions yielded 4.0 mg of product as an oil (quantitative).

CIMS: m/e 312.0 $(M + H)^+$, 336.1 $(M + Na)^+$, 351.0 $(M + K)^+$.

^{1}H NMR: (D_2O, 500 MHz) δ 4.77 (0.3 H, d, J = 8.8 Hz), 4.66 (0.7H, dd, J = 1.7, 10.7 Hz), 4.55 (0.7H, d, J = 9.2 Hz), 4.50 (0.3 H, d, J = 9.3 Hz), 4.34−4.28 (1H, m), 4.06 (0.7 H, dd, J = 5.6, 12.0 Hz), 4.01 (0.7 H, d, J = 12.0 Hz), 3.83−3.78 (1.3 H, m), 3.75 (0.3 H, td, J = 2.1, 5.1 Hz), 3.31, 3.07 (1H, 2 dd, J = 5.8, 15.4 Hz, J = 4.3, 16.0 Hz), 2.90−2.74 (1H, m), 2.74 (3H, s), 2.82, 2.48 (1H, 2dd, J = 6.8, 16.0 Hz, J = 10.1, 15.5 Hz), 2.46, 2.43 (1H, 2d, J = 13.8 Hz, J = 14.5 Hz), 2.30−2.10 (2H, m), 2.19, 2.17 (3H, 2s), 1.97−1.84 (2H, m).

Ac-Hel_1-Gly-OH. To a chilled solution of Ac-Hel_1-OH (3.9 mg, 13 μmol), H-Gly-O-t-Bu·HCl (3.2 mg, 19 μmol), and HOBt (3.0 mg, 20 μM) in DMF (300 μL) were added DIEA (3.0 μL, 17 μmol) and 1-(3-(dimethylamino)propyl)-3-ethylcarbodiimide hydrochloride (3.3 mg, 17 μmol). After 1 h at 0 °C and 1 deg at 25 °C the solution was evaporated, and the residue was taken up in MeCN/H_2O and purified by preparative HPLC (0→40% MeCN(H_2O with 0.1% TFA)/linear gradient/20 min, RT 16.8 min). Evaporation of the appropriate fractions gave a residue that was dissolved in DCM (2 mL) at 0 °C and treated with TFA (4 mL). After 2 h at 0 °C the solution was evaporated, and the residue was purified by preparative HPLC (5→43% MeCN(H_2O with 0.1% TFA)/20 min, RT 10.3 min). Evaporation of the appropriate fractions gave the title compound as a colorless oil, 4.4 mg, 95%.

Analytical HPLC: 7% MeCN(93% H_2O with 0.1% TFA)/isocratic, RT 11.6 min.

CIMS: m/e 357.0 $[M + H]^+$ 379.3 $[M + Na]^+$.

^{1}H NMR (9:1 H_2O−D_2O, 500 MHz) δ 8.44 (0.4 H, t, J = 5.3 Hz), 7.92 (0.6H, t, J = 5.4 Hz), 4.68 (0.4H, d, J = 10.4 Hz), 4.61 (0.6H, d, J = 8.5 Hz), 4.37−4.29 (1H, m), 4.09−4.03 (1.6H, m), 4.01 (1.6H, d, J = 12.0 Hz), 3.96, 3.93 (1H, 2 t, J = 5.9 Hz), 3.83−3.78 (1.4 H, m), 3.77−3.74 (0.4 H, m), 3.32, 3.13 (1H, 2 dd, J = 5.8, 15.5 Hz, J = 4.6, 16.0 Hz), 2.89−2.81 (1H, m), 2.79, 2.50 (1H, 2 dd, J = 7.4, 16.1 Hz, J = 10.2, 15.5 Hz), 2.47, 2.43 (1H, 2 d, J = 13.6 Hz, J = 14.6 Hz), 2.27 − 2.14 (2 H, m), 2.18, 2.16 (3H, 2s), 2.03−1.98 (1H, m), 1.94−1.86 (1H, m).

Ac-Hel_1-G_3-OH. Cbz-Gly-Gly-Gly-O-t-Bu (17 mg, 53 μmol) was dissolved in EtOH (10 mL) and hydrogenated (50 psi H_2) with Pd black (21 mg) for 6 h. After filtration through Celite and solvent removal, the residue was dissolved in dry DMF (0.75 mL). To the 0 °C solution was added Ac-Hel_1-OH (10 mg, 34 μmol), HOBt (10 mg, 64 μM), and 1-(3-(dimethylamino)propyl)-3-ethylcarbodiimide hydrochloride (18 mg, 96 μmol). After 1 h at 0 °C and 1 day at 25 °C the solution was evaporated, and the residue was taken up in MeCN/H_2O and purified by preparative HPLC (5→100% MeCN(H_2O with 0.1% TFA/gradient)/25 min, RT 8.6 min). Evaporation of the appropriate fractions gave a residue (13 mg, 72%) that was dissolved in DCM (4 mL) at 0 °C and treated with TFA (4 mL). After 1 h at 0 °C the solution was evaporated, and the residue was purified by preparative HPLC (5→10% MeCN-(H_2O with 0.1% TFA)/linear gradient/20 min, RT 12.0 min). Evaporation of the appropriate fractions gave the title compound as a colorless oil, 10 mg, 89% from the ester.

^{1}H NMR (9:1 H_2O−D_2O, 500 MHz) δ 8.58 (0.4H, t, J = 5.8 Hz), 8.30−8.25 (0.8H, m), 8.22 (0.6H, t, J = 5.7 Hz), 8.16 (0.6H, t, J = 5.7 Hz), 8.05 (0.6H, t, J = 5.8 Hz), 4.74, 4.68 (1H, 2d, J = 8.9 Hz, J = 10.4 Hz), 4.60−4.58 (1H, m), 4.37, 4.31 (1H, 2 dt, J = 4.3, 6.9 Hz, J = 6.1, 10.2 Hz), 4.08−3.94 (6.6 H, m), 3.83−3.79 (1.4H, m), 3.76 (0.4H, td, J = 2.1, 5.0 Hz), 3.32, 3.13 (1H, 2dd, J = 5.9, 15.5 Hz, J = 4.5, 16.0 Hz), 2.89−2.82 (1H, m), 2.80, 2.50 (1H, 2dd, J = 7.3, 15.9 Hz, J = 10.1, 15.5 Hz), 2.47, 2.43 (1H, 2d, J = 13.5 Hz, J = 14.5 Hz), 2.30−2.17 (2H, m), 2.17, 2.14 (3H, 2s), 2.03−1.87 (2H, m).

Ac-Hel_1-G_5-OH. Following the procedure analogous to that given above for the conversion of Ac-Hel_1-OH to Ac-Hel_1-Gly_3-OH, Ac-Hel_1-OH was coupled with H-Gly-Gly-O-t-Bu to yield Ac-Hel_1-Gly_2-OH, preparative HPLC (5→100% MeCN(H_2O with 0.1% TFA)/linear gradient/20 min, RT 13.0 min), which was coupled with H-Gly_3-O-t-Bu, and the resulting ester was cleaved with TFA to yield the title compound, preparative HPLC (5→100% MeCN(H_2O with 0.1% TFA)/exponential gradient/20 min, RT 12.6 min).

CIMS: m/e 584.3 $[M + H]^+$ 604.4 $[M + Na]^+$ 622.6 $[M + K]^+$.

^{1}H NMR (9:1 H_2O−D_2O, 500 MHz) δ 8.57 (0.4 H, t, J = 5.8 Hz), 8.42 (0.4H, t, J = 5.8 Hz), 8.39−8.34 (2H, m), 8.32−8.25 (1H, m), 8.18 (0.6H, t, J = 6.0 Hz), 8.05 (0.6H, t, J = 6.0 Hz), 4.77 (0.4H, d, J = 8.9 Hz), 4.68 (0.6H, d, J = 10.5 Hz), 4.61−4.57 (1H, m), 4.37 (0.6H, td, J = 4.6, 6.8 Hz), 4.31 (0.4H, dt, J = 6.0, 10.2 Hz), 4.08−3.95 (11.2H, m), 3.83−3.79 (1.4H, m), 3.75 (0.4H, td, J = 2.2, 5.2 Hz), 3.32, 3.12 (1H, 2dd, J = 5.8, 15.5 Hz, J = 4.6, 16.0 Hz), 2.89−2.82 (1H, m), 2.80, 2.50 (1H, 2dd, J = 7.5, 16.1 Hz, J = 10.1, 15.5 Hz), 2.47, 2.43 (1H, 2d, J = 13.7 Hz, J = 14.5 Hz), 2.30−2.17 (2H, m), 2.17, 2.14 (3H, 2s), 2.02−1.86 (2H, m).

Ac-Hel_1-G_6-OH. Following the procedure analogous to that given above for the conversion of Ac-Hel_1-OH to Ac-Hel_1-G_3-OH, Ac-Hel_1-G_3-OH was coupled with H-Gly-Gly-Gly-O-t-Bu to yield Ac-Hel_1-Gly_6-O-t-Bu, preparative HPLC (5→100% MeCN(H_2O with 0.1% TFA)/linear gradient/25 min, RT 9.0 min). The ester was cleaved with TFA to yield the title compound as an oil, 95%, preparative HPLC (5→100% MeCN(H_2O with 0.1% TFA)/exponential gradient/20 min, RT 11.0 min).

CIMS: m/e 641.4 $[M + H]^+$ 665.2 $[M + Na]^+$.

^{1}H NMR (9:1 H_2O−D_2O, 500 MHz) δ 8.57 (0.4H, t, J = 6.0 Hz), 8.43−8.25 (4.4H, m), 8.19 (0.6H, t, J = 5.9 Hz), 8.06 (0.6H, t, J = 6.1 Hz), 4.77 (0.4H, d, J = 9.0 Hz), 4.68 (0.6H, d, J = 10.4 Hz), 4.61−4.58 (1H, m), 4.37 (0.6H, td, J = 4.7, 6.8 Hz), 4.31 (0.4H, dt, J = 6.0, 10.2 Hz), 4.08−3.95 (13.2H, m), 3.83−3.79 (1.4H, m), 3.75 (0.4H, td, J = 2.1, 5.1 Hz), 3.32, 3.13 (1H, 2dd, J = 5.8, 15.5 Hz, J = 4.6, 16.0 Hz), 2.89−2.80 (1H, m), 2.80, 2.50 (1H, 2dd, J = 7.6,

16.2 Hz, J = 10.1, 15.4 Hz), 2.47−2.43 (1H, 2d, J = 13.5 Hz, J = 14.5 Hz), 2.30−2.12 (2H, m), 2.17, 2.14 (3H, 2s), 2.02−1.86 (2H, m).

Ac-Hel$_1$-Ala$_2$-Leu-Ala$_3$-OH and Ac-Hel$_1$-Ala$_2$-Gly-Ala$_3$-OH. General Procedure for the Preparation of Ac-Hel$_1$-Ala$_2$-Xxx-Ala$_3$-OH. Cbz-Ala-Ala-Xxx-O-*t*-Bu, prepared by 1-(3-(dimethylamino)propyl)-3-ethylcarbodiimide hydrochloride/HOBt coupling of Cbz-Ala-Ala-OH with H-Xxx-O-*t*-Bu was hydrogenated as described in the above procedures to yield H-Ala-Ala-Xxx-O-*t*-Bu. This compound (1.5 equiv) in DMF was coupled (0 °C, then 25 °C) with Ac-Hel$_1$-OH (1.0 equiv), in the presence of HOBt (1.6 equiv) and 1-(3-(dimethylamino)propyl)-3-ethylcarbodiimide hydrochloride (2.0 equiv). After 1 h at 0 °C and 1 day at 25 °C the solution was evaporated, and the residue was taken up in MeCN/H_2O and purified by preparative HPLC (5→100% MeCN (H_2O with 0.1% TFA)/linear gradient/25 min, RT Leu 14.3 min; RT Gly 9.2 min). Evaporation of the appropriate fractions gave a residue that was dissolved in DCM at 0 °C and treated with TFA as described for preparation of Ac-Hel$_1$-Gly$_3$-OH. After 2 h at 0 °C the solution was evaporated, and the residue was purified by preparative HPLC (5→100% MeCN(H_2O with 0.1% TFA)/linear gradient/20 min, RT Leu 19.0 min; RT Gly HPLC (10→100% MeCN(H_2O with 0.1% TFA)/linear gradient/15 min, 5.3 min)). Evaporation of the appropriate fractions gave the tripeptide conjugates as oils in yields of 47−69% based on Ac-Hel$_1$-OH.

Coupling of Ac-Hel$_1$-A$_2$-X-OH (1.0 equiv) with H-A$_3$-O-*t*-Bu (1.6 equiv) in DMF with HOBt (2.0 equiv) and 1-(3-(dimethylamino)-propyl)-3-ethylcarbodiimide hydrochloride (2.1 equiv) in the usual manner gave after evaporation of solvent and purification by preparative HPLC (5→100% MeCN(H_2O with 0.1% TFA)/linear gradient/20 min) the desired hexapeptide esters, RT Leu 12.6 min and RT Gly 9.0 min. Cleavage by TFA of the ester group in the usual manner gave the title compounds after purification by preparative HPLC (5→100% MeCN-(H_2O with 0.1% TFA)/exponential gradient/20 min, RT Leu 18.6 min; RT Gly 16.5 min).

Ac-Hel$_1$-A$_2$-L-A$_3$-OH. Analytical HPLC: 10→100% MeCN(H_2O with 0.1% TFA)/linear gradient/20 min, RT 17.7 min.

CIMS: *m/e* 767.0 $[M + H]^+$ 790.1 $[M + Na]^+$ 806.2 $[M + K]^+$.

^{1}H NMR (9:1 H_2O−D_2O, 500 MHz) δ 8.41 (0.3H, d, J = 5.1 Hz), 8.29 (0.3H, d, J = 5.5 Hz), 8.27 (0.3H, d, J = 6.6 Hz), 8.15−8.12 (1.3H, m), 8.08 (0.3H, d, J = 7.1 Hz), 7.95 (0.7H, d, J = 6.1 Hz), 7.93 (0.7H, d, J = 5.6 Hz), 7.87 (0.7H, d, J = 6.5 Hz), 7.81 (0.7H, d, J = 5.5 Hz), 7.61 (0.7H, d, J = 6.3 Hz), 4.75, 4.70 (1H, 2d, J = 8.8 Hz, J = 10.8 Hz), 4.56, 4.54 (1H, 2 d, J = 11.8 Hz, J = 10.2 Hz), 4.42 (0.7H, dq, J = 4.1, 6.6 Hz), 4.39−4.20 (6.3H, m), 4.09, 3.82 (1H, 2 dd, J = 5.7, 12.1 Hz), 4.05−3.81 (1H, 2 d, J = 12.0 Hz), 3.82, 3.75 (1H, 2 td, J = 1.4, 4.9 Hz), 3.31, 3.06 (1H, 2 dd, J = 5.8, 15.5 Hz, J = 4.2, 16.0 Hz), 2.94−2.82 (1H, m), 2.88, 2.50 (1H, 2dd, J = 6.9, 16.1 Hz, J = 10.1, 15.5 Hz), 2.47, 2.44 (1H, 2d, J = 13.6 Hz, J = 14.8 Hz), 2.28−2.19 (2H, m), 2.19, 2.14 (3H, 2s), 2.00−1.88 (2H, m), 1.71−1.59 (3H, m), 1.46−1.36 (15H, m), 0.94−0.92 (3H, 2d, J = 6.0 Hz, J = 5.5 Hz), 0.89, 0.88 (3H, 2d, J = 6.2 Hz).

Ac-Hel$_1$-A$_2$-G-A$_3$-OH. Anal. HPLC: 10→100% MeCN(H_2O with 0.1% TFA)/linear gradient/20 min, RT 14.8 min.

CIMS: *m/e* 712.0 $[M + H]^+$ 734.4 $[M + Na]^+$ 750.9 $[M + K]^+$.

^{1}H NMR (D_2O, 500 MHz) δ 4.75, 4.69 (1H, 2d, J = 8.8 Hz, J = 1.4, 10.8 Hz), 4.58, 4.54 (1H, m), 4.41−4.24 (6H, m), 4.07 (0.6H, dd, J = 5.5, 12.1 Hz), 4.03 (0.6H, dd, J = 12.0 Hz), 3.97−3.89 (2H, m), 3.86−3.77 (1.4H, m), 3.31, 3.08 (1H, 2 dd, J = 5.8, 15.4 Hz, J = 4.3, 16.0 Hz), 2.90−2.81 (1H, m), 2.52, 2.49 (1H, 2dd, J = 7.1, 15.9 Hz, J = 10.2, 15.4 Hz), 2.46, 2.42 (1H, 2d, J = 13.6, J = 14.6 Hz), 2.26−2.16 (2H, m), 2.18, 2.14 (3H, 2s), 2.01−1.82 (2H, m), 1.44−1.39 (15H, m).

Ac-Hel$_1$-L-Lac-OH. To a solution of Ac-Hel$_1$-OH (18.8 mg, 63.1 μmol) and 4-DMAP (32.2 mg, 264 μmol) in dry pyridine (500 μL) at 0 °C was added carbonyldiimidazole (35.4 mg, 218 μmol), followed by methyl (L)-lactate (500 μL). The mixture was allowed to stir for 1 h at 0 °C and for 2 days at 23 °C and then treated with carbonyldiimidazole (21 mg, 130 μmol) and stirred for 2 days. Evaporation yielded an oil that was purified by preparative HPLC (8→50% MeCN-(water with 0.1% TFA)/linear gradient/15 min, RT 13.2 min). The diester was obtained as an oil (17 mg, 69%), FABMS *m/e* 385.3 $[M + H]^+$.

The diester (17 mg, 44 μmol) was selectively saponified by 0.1 M aqueous NaOH (460 μL) for 8 h at 25 °C. Acidification and purification by preparative HPLC (8→50% MeCN (H_2O with 0.1% TFA)/exponential gradient/20 min, RT 19.0 min) and evaporation of the appropriate fractions gave the title compound as a white foam, 13 mg, 78%.

Analytical HPLC: 8→50% MeCN(H_2O with 0.1% TFA)/linear gradient/15 min, RT 13.5 min.

^{1}H NMR (D_2O, 500 MHz) δ 5.13, 5.13 (1H, 2 q, J = 7.1 Hz), 4.79, 4.71 (1H, 2 d, J = 8.6 Hz), 4.68−4.58 (1H, 2 d, J = 9.0 Hz), 4.37, 4.32 (1H, 2dq, J = 5.9, 9.2 Hz, J = 6.1, 10.2 Hz), 4.03, 3.82 (1H, 2 dd, J = 5.9, 12.3 Hz), 3.97, 3.82 (1H, 2 d, J = 12.2 Hz), 3.79−3.75 (1H, m), 3.43, 3.33 (1H, 2 dd, J = 5.9, 15.6 Hz, J = 6.0, 15.5 Hz), 2.86, 2.75 (1H, 2 qd, J = 5.2, 9.1, 13.6 Hz, J = 13.8 Hz), 2.58, 2.51 (1H, 2 dd, J = 9.3, 15.7 Hz), 2.47, 2.37 (1H, 2 d, J = 13.6 Hz, J = 13.8 Hz), 2.29−2.08 (3H, m), 2.15, 2.14 (3H, 2s), 1.94−1.89 (1H, m), 1.55, 1.54 (3H, 2 d, J = 7.1 Hz).

Ac-Hel$_1$-L-Lac-Ala$_2$-OH. To a solution in dry DMF (0.5 mL) of Ac-Hel$_1$-L-Lac-OH (13 mg, 34 μmol), H-A-A-O-*t*-Bu (prepared by hydrogenation of 21 mg, 60 μmol, of Cbz-Ala-Ala-O-*t*-Bu), and HOBt (7.2 mg, 47 μmol) at 0 °C was added 1-(3-(dimethylamino)propyl)-3-ethylcarbodiimide hydrochloride (10.3 mg, 54 μmol). After 40 min at 0 °C and 24 h at 23 °C the solvent was evaporated and the residue was subjected to purification by preparative HPLC (5→50% MeCN(H_2O with 0.1% TFA)/linear gradient/15 min, RT 14.6 min). Evaporation of the appropriate fractions gave a residue that was dissolved in DCM (1 mL) at 0 °C and treated with TFA (2 mL) and anisole (50 μL). After 1 h at 0 °C the solution was evaporated, and the residue was purified by preparative HPLC: 2→50% MeCN(H_2O with 0.1% TFA)/exponential gradient/15 min, RT 15.0 min.

^{1}H NMR (9:1 H_2O−D_2O, 500 MHz) δ 8.44, 8.36 (1H, 2 d, J = 6.0 Hz, J = 6.7 Hz), 8.18, 8.14 (1H, 2 d, J = 6.1 Hz, J = 6.6 Hz), 5.09, 5.08 (1H, 2 q, J = 7.0 Hz), 4.67, 4.59 (1H, 2 d, J = 9.4 Hz, J = 8.7 Hz), 4.42−4.27 (4H, m), 4.05, 3.82 (1H, dd, J = 6.0, 12.2 Hz), 4.00, 3.82 (1H, d, J = 12.2 Hz), 3.80, 3.76 (1H, 2 td, J = 5.7 Hz, J = 2.1, 5.1 Hz), 3.33, 3.26 (1H, 2 dd, J = 5.9, 15.4 Hz, J = 5.3, 15.7 Hz), 2.86, 2.80 (1H, 2qd, J = 5.1, 9.0, 13.6 Hz, J = 6.0, 10.0, 16.0 Hz), 2.68, 2.51 (1H, 2 dd, J = 8.6, 15.7 Hz, J = 10.1, 15.4 Hz), 2.47, 2.39 (1H, 2 d, J = 13.7 Hz, J = 14.1 Hz), 2.29−2.18 (2H, m), 2.18, 2.15 (3H, 2s), 2.11−2.04 (1H, m), 1.94−1.91 (1H, m), 1.50, 1.49 (3H, 2 d, J = 7.0 Hz), 1.43, 1.42, 1.41, 1.40 (6 H, 4 d, J = 7.3 Hz).

Ac-Hel$_1$-L-Lac-Ala$_5$-OH. To a solution in dry DMF (1.0 mL) of Ac-Hel$_1$-L-Lac-A$_2$-OH (10 mg, 20 μmol), H-A-A-A-O-*t*-Bu (prepared by hydrogenation of 14 mg, 32 μmol, of Cbz-Ala$_3$-O-*t*-Bu), and HOBt (5.0 mg, 33 μmol) at 0 °C was added 1-(3-(dimethylamino)propyl)-3-ethylcarbodiimide hydrochloride (6.8 mg, 36 μmol). After 1 h at 0 °C and 24 h at 23 °C the solvent was evaporated and the residue was subjected to purification by preparative HPLC: 5→100% MeCN(H_2O with 0.1% TFA)/linear gradient/20 min, RT 10.6 min. Evaporation of the appropriate fractions gave a residue that was dissolved in DCM (2 mL) at 0 °C and treated with TFA (4 mL). After 2 h at 0 °C the solution was evaporated, and the residue was purified by preparative HPLC: 5→100% MeCN(H_2O with 0.1% TFA)/exponential gradient/20 min, RT 17.6 min.

FABMS: *m/e* 726.6 $[M + H]^+$ 749.1 $[M + Na]^+$ $(M + K)^+$.

^{1}H NMR (9:1 H_2O−D_2O, 500 MHz) δ 8.39 (0.4H, d, J = 5.8 Hz), 8.30 (0.4H, d, J = 6.6 Hz), 8.22 (0.6H, d, J = 5.8 Hz), 8.19 (0.4H, d, J = 6.1 Hz), 8.15 (0.8H, d, J = 5.1 Hz), 8.10 (0.6H, d, J = 6.5 Hz), 7.91 (0.6H, d, J = 5.1 Hz), 7.88 (0.6H, d, J = 6.1 Hz), 7.75 (0.6H, d, J = 5.8 Hz), 5.10, 5.02 (1H, 2 q, J = 6.9 Hz, J = 7.1 Hz), 4.74, 4.71 (1H, 2 d, J = 10.2 Hz), 4.66, 4.63 (1H, 2 d, J = 9.4 Hz, J = 9.1 Hz), 4.45 (0.6H, dt, J = 4.3, 7.4 Hz), 4.39−4.21 (5.4H, m), 4.10, 3.82 (1H, dd, J = 6.1, 12.1 Hz), 4.05, 3.76 (1H, d, J = 12.1 Hz), 3.33, 3.14 (1H, dd, J = 5.9, 15.6 Hz), 2.48, 2.42 (1H, d, J = 13.6 Hz, J = 14.5 Hz), 2.37−2.20 (2H, m), 2.17, 2.13 (3H, 2s), 2.11, 2.05 (1H, 2dd, J = 5.0, 11.8 Hz, J = 6.1, 12.6 Hz), 1.97, 1.92 (1H, 2 dd, J = 5.9, 12.5 Hz, J = 5.3, 11.8 Hz), 1.50, 1.49 (3H, 2 d, J = 7.0 Hz), 1.45−1.37 (15 H, m).

Solid-Phase Peptide Synthesis of Peptides with C-Terminal Amides. All syntheses were carried out using an N-α-Fmoc protection strategy. Although the deprotection/acylation cycles proceeded cleanly with a normal synthetic protocol through the first five steps of the

Table 3. Characterizing Information for Ac-Hel$_1$-Peptide Conjugates

sequence	HPLC ret time[a] (min)	mol wt	mass spectrometry[b]
AAGAAA-OH	14.80	710.31	712.0 (M + H), 734.4 (M + Na), 750.9 (M + K)
AALAAA-OH	17.66	766.38	767.0 (M + H), 790.1 (M + Na), 806.2 (M + K)
Lac-AAAAA-OH	17.6[c]	725.31	726.6 (M + H), 749.1 (M + Na), 765.5 (M + K)
NHMe	see text	311.13	312.2 (M + H), 336.1 (M + Na), 351.0 (M + K)
G-OH	see text	355.12	357.0 (M + H), 379.3 (M + Na)
GGGGGG-OH	see text	640.23	641.4 (M + H), 365.2 (M + Na)
AALAAAAK-NH_2	17.96	965.52	967.9 (M + H), 990.0 (M + Na)
AAFAAAAK-NH_2	18.13	999.51	1001.1 (M + H), 1024.5 (M + Na)
AAIAAAAK-NH_2	17.96	965.52	967.4 (M + H)
AAVAAAAK-NH_2	17.43	951.51	952.2 (M + H)
AAGAAAAK-NH_2	15.05	909.46	909.2 (M + H)
AAAAAAAK-NH_2	16.06	923.48	924.0 (M + H)
AAKAAAAK-NH_2	14.76	981.54	981.3 (M + H)
AAOrnAAAAK-NH_2	14.60	967.53	966.3 (M + H)
AARAAAAK-NH_2	15.23	1009.54	1010.4 (M + H)
AAMAAAAK-NH_2	17.46	983.48	983.7 (M + H)
AAYAAAAK-NH_2	17.00	1015.50	1015.8 (M + H)
AASAAAAK-NH_2	15.30	939.47	940.4 (M + H)
AATAAAAK-NH_2	15.56	953.49	953.8 (M + H)
AAQAAAAK-NH_2	15.60	980.50	981.9 (M + H)
AANAAAAK-NH_2	14.93	966.48	966.0 (M + H)
AADAAAAK-NH_2	15.16	967.47	967.4 (M + H)
AAHAAAAK-NH_2	14.86	990.51	989.7 (M + H)
AAAAAAKA-NH_2	17.20	923.48	923.5 (M + H)
AAAAAKAA-NH_2	18.10	923.48	923.4 (M + H)
AAAAAKAAA-NH_2	18.03	994.51	995.8 (M + H)
AAAKAAAA-NH_2	17.20	923.48	923.8 (M + H)
AAKAAAAA-NH_2	15.73	923.48	923.3 (M + H)
AAAAA-Orn-NH_2	15.13	767.39	767.4 (M + H)
AAAAA-DLys-NH_2	16.53	781.40	781.6 (M + H)
AAAAA-R-NH_2	16.00	809.40	809.0 (M + H)
AAAAA-Nle-NH_2	18.16	765.38	766.5 (M + H), 788.4 (M + Na)
AALLAAA-NH_2	19.50	1007.57	1007.9 (M + H)
AAALAAA-NH_2	17.63	965.52	965.6 (M + H)
AAIIAAA-NH_2	19.03	1007.57	1007.8 (M + H)
AAAIAAA-NH_2	17.66	965.52	965.6 (M + H)
AAFFAAA-NH_2	19.76	1075.54	1075.2 (M + H)
AAAFAAA-NH_2	18.06	999.51	998.5 (M + H)
AAFLAAA-NH_2	19.73	1041.55	1042.3 (M + H)
AAFIAAA-NH_2	19.60	1041.55	1042.3 (M + H)
AAELAAA-NH_2	17.36	1023.53	1023.5 (M + H)
AALTAAA-NH_2	17.76	995.53	995.0 (M + H)
AATLAAA-NH_2	17.36	995.53	995.2 (M + H)
AA-Nle-AAAA-NH_2	18.16	965.52	965.7 (M + H)
AA-Nve-AAAA-NH_2	17.46	951.51	952.4 (M + H)
AA-Abu-AAAA-NH_2	16.76	937.49	937.9 (M + H)
AA-DAla-AAAA-NH_2	15.23	937.49	937.5 (M + H)
AA-Tle-AAAA-NH_2	17.70	965.52	965.1 (M + H)
AAAK-NH_2	13.40	639.33	649.8 (M + H)
AAAAK-NH_2	14.60	710.37	710.5 (M + H)
AAAAAK-NH_2	15.26	781.40	781.7 (M + H)
AAAAAAK-NH_2	15.70	852.44	852.8 (M + H)
AAAAAAAAK-NH_2	16.60	994.51	994.2 (M + H)

[a] 10→100% MeCN (H_2O with 0.1% TFA), linear gradient/20 min/analytical HPLC. [b] Plasma desorption MS. [c] 5→100% MeCN (H_2O with 0.1% TFA), linear gradient/20 min/analytical HPLC.

syntheses of homo-alanine oligomers, HPLC analysis of intermediates at later stages in the synthesis identified impurities arising from a combination of incomplete deprotection and acylation steps. Similar problems with alanine-rich peptides have been reported.[39] Elevated deprotection times and temperatures together with multiple acylations resolved this problem. The final purity of products obtained by the revised protocol averaged >95% as judged by HPLC, mass spectroscopy, and NMR analysis. The synthesis technique was validated by tests in which gradient elutions on an analytical HPLC sufficed to separate amino-terminus-deblocked peptides as well as template–peptide conjugates that differed in length by one alanine residue.

All SPPS was carried out either in glass solid-phase vessels silanized with Sigmacote or in polyethylene cartridges supplied by Dupont for the RaMPS multiple peptide synthesis system. Amino acids were blocked by α-Fmoc and *tert*-butyl side chain protection.[40] An aminomethyl resin (1% cross-linked polystyrene–divinyl benzene, 0.9 mmol/g loading level) was functionalized with the Knorr linker, Fmoc 2,4-dimethoxy-4′-(carboxymethyloxy)benzhydrylamine. Deprotection was carried out with piperidine, and acylation was performed with preformed pentafluorophenyl esters for Ser, Thr, Asp, Glu, Asn, Gln, and Lys or with free acids activated by pyBOP/HOBt/DIEA for all other cases.[41] Products of asparagine couplings by MS were free of dehydration byproducts, and methionine products contained less than 3% sulfoxide. The τ-imidazole site of histidine was blocked with

(39) Merrifield, R. B.; Singer, B. T. *Anal. Biochem.* **1988**, *174*, 399–414. Thaler, A.; Seebach, D.; Cardinaux, F. *Helv. Chim. Acta* **1991**, *74*, 628–643.

(40) Sheppard, R. C.; Williams, B. J. *J. Chem. Soc., Chem. Commun.* **1982**, *11*, 587–589. Meienhofer, J. In *Chemistry and Biochemistry of the Amino Acids*; Barrett, G. C., Ed.; Chapman and Hall: London, 1985; pp 297–337.

(41) Coste, J.; Le-Nguyen, D.; Castro, B. *Tetrahedron Lett.* **1990**, *31*, 205–208.

N-trityl[42] and the guanidino function of Arg was blocked with the 2,2,5,7,8-pentamethylchroman-6-sulfonyl (Pmc) group.[43]

Functionalization of the aminomethyl resin was carried out after 3 × 2 min DCM washes, a 24 h DCM preswelling step, and treatment with 2.5% DIEA in DCM (1 × 15 min), followed by DCM washes (3 × 5 min) and 1:1 DCM−DMF washes (3 × 5 min). Treatment with a 0.18 M solution of 1.5 equiv of Knorr linker in 1:1 DCM−DMF containing 1.4 equiv of HOBt and 1.6 equiv of DIC was followed by reagent removal by washing with DCM−DMF (3 × 5 min) followed by DCM (3 × 5 min).

Solutions of acylating agents were freshly prepared in all cases either as 1.5−2.0 mL in DMF of 2.5 equiv of the appropriate PFP ester (0.1−0.2 M) together with 2.5 equiv of HOBt, or as 1.5−2.0 mL of a solution in DMF of 2.5 equiv of the respective blocked amino acid (0.1−0.2 M), 2.5 equiv of HOBT, 3 equiv of pyBOP, and 4−5 equiv of DIEA. The first acylation of the functionalized resin was carried out by washing the resin with 1:1 DCM−DMF (3 × 2 min) and DMF (6 × 2 min), followed by deprotection with 1:1 piperidine in DMF (1 × 5 min, then 1 × 20 min), washing with DMF (10 × 2 min), and treatment with the acylating solution (1 × 2.5 h). Reagents were removed by washing with DMF (6 × 2 min) and DCM (3 × 2 min). The acylation step was usually monitored for completeness by the Kaiser ninhydrin test. The second through fourth acylation steps were identical to the first except for omission of the initial washing steps with 1:1 DCM−DMF and use of longer deprotection conditions (30 min). The acylation time was extended to 4 h if the ninhydrin test after 2.5 h was positive. The fifth through tenth acylations were carried out with the following changes: The piperidine solution used in deblocking was heated to 60 °C immediately before addition to the reaction vessel and the second piperidine contact was allowed to proceed for 30 min. After the first acylation step, the solution was flushed from the reaction vessel, the resin was washed with DMF (6 × 2 min), and a second acylation under identical conditions was performed (2.5−4 h). For final acylation with Ac-Hel$_1$-OH, the acylation protocol was identical except that the amino acid-derived acylating agent was replaced with an 0.7-mL solution of Ac-Hel$_1$-OH (0.5 equiv) in DMF containing HOBt and pyBOP (0.5 equiv each).

Cleavage of the peptide conjugate from the resin was carried out through contact with a freshly prepared mixture of 90% TFA/5% H_2O/5% thioanisole (1 mL). The resin was treated for 45 min at 25 °C, the solution was filtered, and this cleavage protocol was repeated. The combined filtrates were collected in a centrifuge tube and treated at 0 °C with diethyl ether (10−15 mL, prefiltered through Al_2O_3, activity grade 0) or methyl *tert*-butyl ether (10−15 mL). Centrifugation at 3000 rpm for 10 min, removal of the supernatant, and resuspension of the pellet in 0 °C ether was followed by recentrifugation. The gel obtained after removal of the supernatant was dried in vacuum overnight, then dissolved and purified by preparative HPLC using MeCN/H_2O (0.1% TFA) as the eluant, with a nonlinear gradient from 10% to 100% MeCN over 20 min. Repurification if necessary resulted in samples estimated to be >95% pure by NMR, HPLC, and MS criteria. HPLC and MS characterizing information is given in Table 3.

Acknowledgment. Financial support from Pfizer Research and from the National Science Foundation, Grant No. 9121702-CHE, is gratefully acknowledged, including funds for the purchase of the Aviv Model 62 DS circular dichroism spectrometer.

JA942970Q

(42) Sieber, P.; Riniker, B. *Tetrahedron Lett.* **1987**, *28*, 6031−6034.
(43) Green, J.; Ogunjobi, O. M.; Ramage, R.; Stewart, A. S. J. *Tetrahedron Lett.* **1988**, *29*, 4341−4344.